Inorganic Chemistry

ARTICLE

pubs.acs.org/IC

Synthesis, Reactivity, and Properties of N-Fused Porphyrin Manganese(I) Tricarbonyl Complexes

Shinya Ikeda, Motoki Toganoh, and Hiroyuki Furuta*

Department of Chemistry and Biochemistry, Graduate School of Engineering, Kyushu University, 744 Moto-oka, Nishi-ku, Fukuoka 819-0395, Japan

Supporting Information

ABSTRACT: The reactions of N-fused tetraphenylporphyrin (NFTPP, **1a**) and its 21-substituted derivatives, 21-Br-NFTPP (**1b**), 21-NO_2-NFTPP (**1c**), and 21-Bz-NFTPP (**1d**), with $Mn(CO)_5Br$ gave the manganese(I) tricarbonyl complexes bearing N-fused tetraphenylporphyrinato ligands (**2a**−**d**), respectively, in 46−99% yields. The complexes were characterized by mass, IR, ^1H and ^{13}C NMR spectroscopy, and the final structural proof was evident from the X-ray crystallographic analysis for **2a**. The crystals of **2a**·CH_2Cl_2 belong to the monoclinic space group $P2_1/n$ (#14), with a = 15.007(2) Å, b = 12.5455(19) Å, c = 21.150(3) Å, β = 102.227(4)°, and Z = 4. The lengths (Å) of three manganese−nitrogen and three manganese−carbon bonds are inequivalent respectively [Mn−N(2), 2.007(2); Mn−N(23), 2.033(2); Mn−N(24), 1.988(3); and Mn−CO, 1.798(4), 1.804(4), 1.841(3)], reflecting the asymmetric structure of the NFp ligand. The aromatic substitution reactions of **2a**, such as nitration, formylation, and chlorination, proceeded without a loss of center metal to give the corresponding 21-nitro (**2c**), 21-formyl (**2e**), and 21-chloro (**2f**) derivatives, regioselectively. In the electrochemical measurements of **2**, one reversible oxidation and two reversible reduction waves were observed. The redox potentials of **2** indicate the narrow energy gaps between the highest occupied molecular orbital and the lowest unoccupied molecular orbital (HOMO−LUMO) being consistent with the electronic absorption spectra that display the absorption edges over 1000 nm. Protonation occurred at the inner core nitrogen of **2a** upon the addition of acids, which is inferred from the ^1H NMR spectra as well as theoretical calculations. By a treatment with amine *N*-oxides, demetalation of **2** proceeded to afford the corresponding NFP free-bases (**1**).

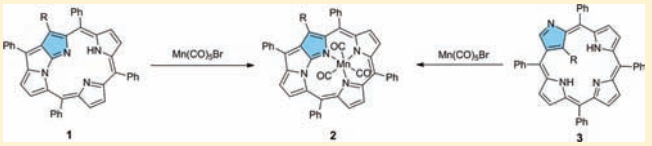

INTRODUCTION

Porphyrin and its analogues have attracted considerable attention because of the versatile properties derived from the characteristic π-system and coordinating metals, which can be used for a broad range of applications.[1] To tune or change the properties, modification of the porphyrin including the framework has been examined extensively, and a large number of porphyrin analogues as well as porphyrin derivatives have been synthesized.[2] Among such porphyrinoids, N-fused porphyrin (NFP)[3] bearing a fused tripentacyclic ring in the core was unexpectedly derived from N-confused porphyrin (NCP).[4] Since then, various fused porphyrinoids, such as N-confused N-fused porphyrin (NC-NFP),[5] doubly N-fused porphyrin (N_2FP),[6] N-fused sapphyrin (NF-Sap),[7] N-fused pentaphyrin (NF-P_5),[8] N-confused, N-fused pentaphyrin (NCF-P_5),[9] and doubly N-fused pentaphyrin (N_2F-P_5),[9] have been prepared, and NFPs form a unique class of porphyrinoid compounds (Chart 1).

NCP has a tetrapyrrolic framework with four *meso* carbon atoms like regular porphyrin; however, the molecule is rather flexible, and ring-inversion of the N-confused pyrrole occurs readily in the macrocyclic framework, which is in marked contrast to the regular porphyrin with rigid and planar structure.[10] Typical examples include the directly linked NCP dimer at the inner carbon atoms of the N-confused pyrrole rings[11] and a bis-iridium NCP complex,[12] both of which contain the inverted N-confused pyrrole ring. Thus, the formation of NFP from NCP could be explained as a consequence of ring-inversion of the N-confused pyrrole ring and subsequent ring fusion in the tetrapyrrolic framework.[3b,10] Interestingly, NFP is converted to NCP in the presence of nucleophiles like alkoxides, where the nucleophiles attack at the C(3)-position of the tripentacyclic ring to induce the ring-opening to afford NCP.[3] This facile interconversion between NCP and NFP is advantageous to the synthesis of a series of NCP and NFP derivatives.[5,6,13]

NFP is an aromatic compound having an [18]annulenic circuit. NFP exhibits a characteristic optical property, in which the absorption maxima at the longest wavelength appear in the near-infrared (NIR) region close to 1000 nm.[3,13,14] The large decrease of the energy gap between the highest occupied molecular orbital and the lowest unoccupied molecular orbital (HOMO−LUMO) in NFP is related to the endocyclic extension of porphyrin π-system, and the trend is further increased with doubly N-fused porphyrin.[6] The corresponding NIR emission of NFP is usually very weak but in some case, like 21-nitro N-fused tetraphenylporphyrin (21-NO_2-NFTPP, **1c**), distinct fluorescence is observed.[14b]

Received: January 7, 2011
Published: June 09, 2011

NFP is expected to form a wide variety of metal complexes as a member of porphyrinoids. Because of the presence of three nitrogen atoms in proximity and one negative charge after deprotonation, NFP could serve as a monoanionic, tridentate nitrogen ligand, which is isoelectronic with cyclopentadienyl (Cp) as well as tris(pyrazolyl)borate (Tp), in the metal coordination.[15] Thus, we can denote the N-fused porphyrinato ligand as NFp to emphasize the similarity to Cp and Tp. The first NFP metal complex was incidentally obtained during the rhenium coordination of N-confused tetraphenylporphyrin (NCTPP, **3a**).[16] Besides the formation of rhenium(I) NCTPP complex, skeleton rearrangement from **3a** to N-fused tetraphenylporphyrin (NFTPP, **1a**) took place to afford the rhenium(I) complex, $Re^{I}(NFTPp)(CO)_3$ (**4a**). Further treatment of **4a** with trimethylamine *N*-oxide afforded the rhenium(VII) complex, $Re^{VII}(NFTPp)O_3$,[17] which catalyzes the deoxygenation reaction of pyridine *N*-oxide derivatives with high turnover numbers.[18] On the other hand, NFP complexes with main group metals have been synthesized by Latos-Grażyński and co-workers (Scheme 1). For example, a phenylboron NFP complex was obtained by the treatment of **1a** with $PhBCl_2$.[19] The same complex was also obtained from the reaction of **3a** with $PhBCl_2$. Interestingly, when NFP or NCP was treated with PCl_3, reduction of the macrocycle and phosphorus insertion proceeded to yield an N-fused isophlorin phosphorus(V) oxo complex.[20] Furthermore, silicon(IV) complexes bearing NFP derivatives were synthesized from NCP.[21]

Encouraged by the success on rhenium(I) complexation, we paid attention toward the manganese ion as the next target. The comparison of two d-block metal complexes in the same group 7 elements could reveal the characteristics of NFp ligand and provide vital information on the NFP complexation. Because the manganese NCP complexes are already known,[22] it would be important to find the conditions with which to afford NFP complexes from NCP (Scheme 2). Herein, we report the synthesis, reactivity, and properties of N-fused porphyrin manganese(I) tricarbonyl complexes (**2**) (Chart 2). Reactions of NFTPP and its 21-substituted derivatives (**1**) gave the manganese(I) tricarbonyl complexes bearing NFp ligands (**2**) in moderate to good yields. Introduction of substituents at the inner carbon of NCP is necessary for these metal-assisted ring fusion reactions. A key role of the substituent at the 21-position

Chart 1. Representative Examples of N-Confused and N-Fused Porphyrinoids

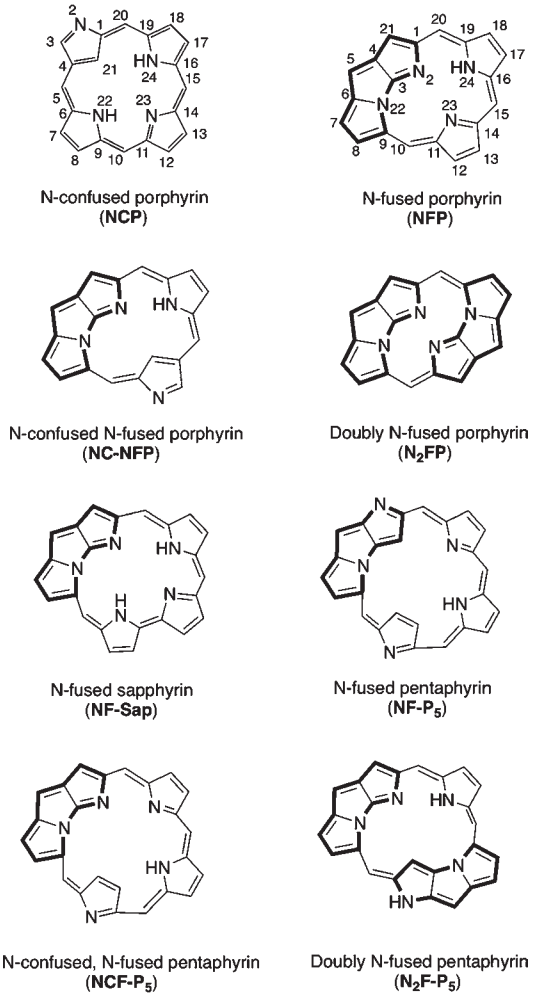

Scheme 1. Formation of NFP Complexes from NFP and NCP

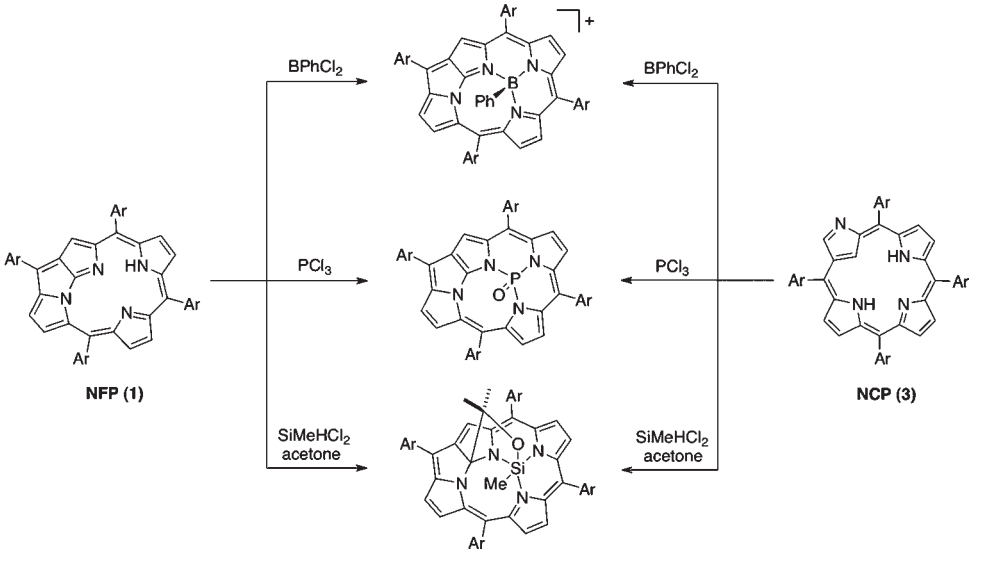

dx.doi.org/10.1021/ic2000393 |*Inorg. Chem.* 2011, 50, 6029–6043

Scheme 2. Reactions of NCP with Group 7 Metals, (a) Re and (b) Mn

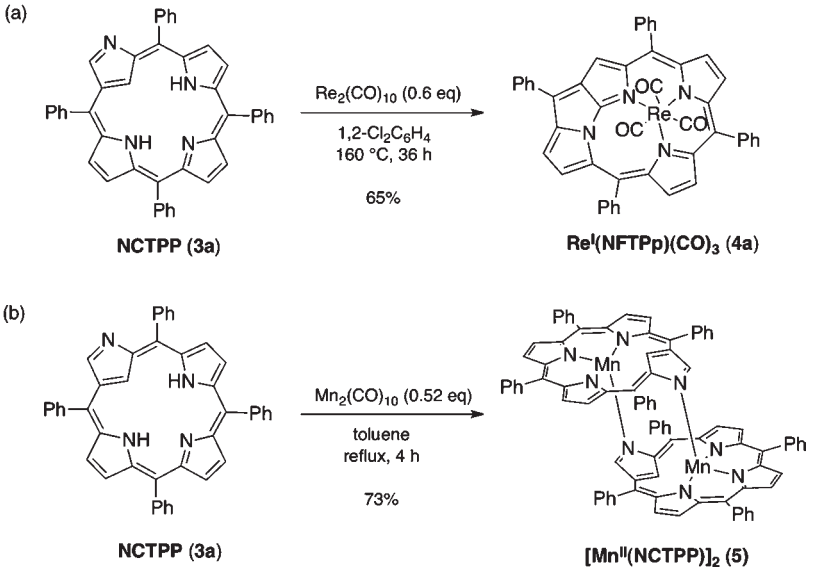

Chart 2. Compounds Structures along with the Numbers Studied in This Work

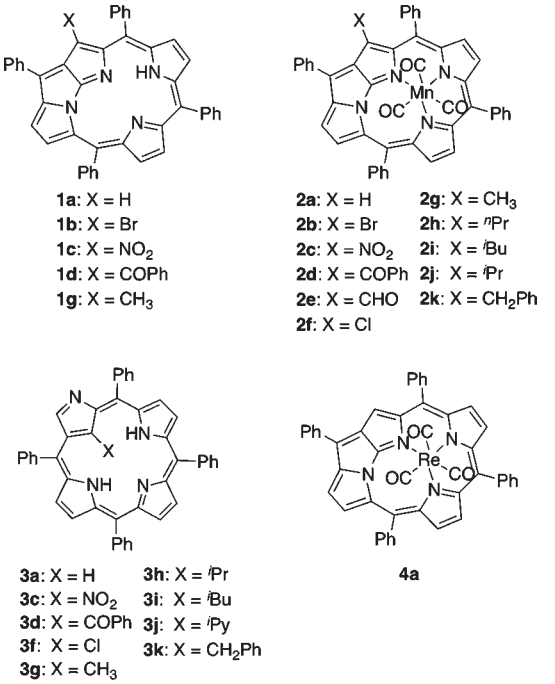

on the ring rearrangement from NCP to NFP and comparison with the rhenium complex are discussed.

Synthesis and Properties of $Mn^I(NFTPp)(CO)_3$ (2a). Synthesis of manganese(I) NFTPP complex ($Mn^I(NFTPp)(CO)_3$, **2a**) was achieved by the reaction of NFTPP (**1a**) with manganese reagents. When a tetrahydrofuran (THF) solution of **1a** and 1.1 equiv of $Mn(CO)_5Br$ in the presence of K_2CO_3 was refluxed for 30 min, manganese complex **2a** was obtained in 88% yield (Scheme 3). In the absence of base, the yield of **2a** decreased substantially (31%).

Scheme 3. Preparation of $Mn^I(NFTPp)(CO)_3$ (2a)

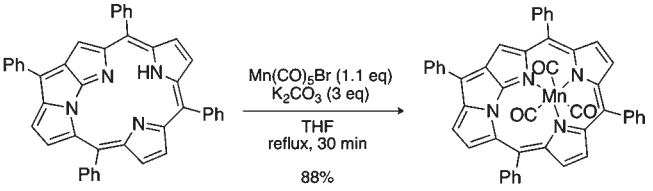

On the other hand, the reaction of **1a** with $Mn_2(CO)_{10}$ also provided **2a** in a moderate yield (56%).

Assignment of the structure of **2a** rested on the ^1H and ^{13}C NMR, mass, and IR spectra, and was subsequently confirmed by X-ray crystallographic analysis. In the mass spectra, the parent ion peak was observed at m/z = 751 (MH^+) in electrospray ionization (ESI) mode, and the reasonable fragment peak was detected at m/z = 666 ($[M - 3(CO)]^+$) in matrix-assisted laser desorption/ionization (MALDI) mode. The ^1H NMR signals appeared in the region from 7.4 to 9.4 ppm, and the spectrum resembled that of **1a** except the disappearance of the singlet signal due to the NH proton. In the ^{13}C NMR spectrum, the signals due to three CO ligands were distinctly observed at 214.08, 216.33, and 216.82 ppm. The strong absorption bands due to the CO stretching were clearly observed at 1902, 1920, and 2005 cm^{-1} in the IR spectrum.[23]

Slow diffusion of hexane into a CH_2Cl_2 solution of **2a** gave violet crystals, and one of them was subjected to X-ray analysis. The crystal structure of **2a** is shown in Figure 1. The apparent molecular shape of **2a** is similar to that of the rhenium(I) complex, $Re^I(NFTPp)(CO)_3$ (**4a**).[16] Namely, the three nitrogen atoms in the core pointing upward to coordinate to the central metal ion, and thus the NFTPp plane is slightly bent with a maximum deviation of 0.573 Å from the mean plane consisting of 24 heavy atoms. The manganese atom is situated above the midst of the three nitrogen atoms. The selected bond lengths and

dx.doi.org/10.1021/ic2000393 |Inorg. Chem. 2011, 50, 6029–6043

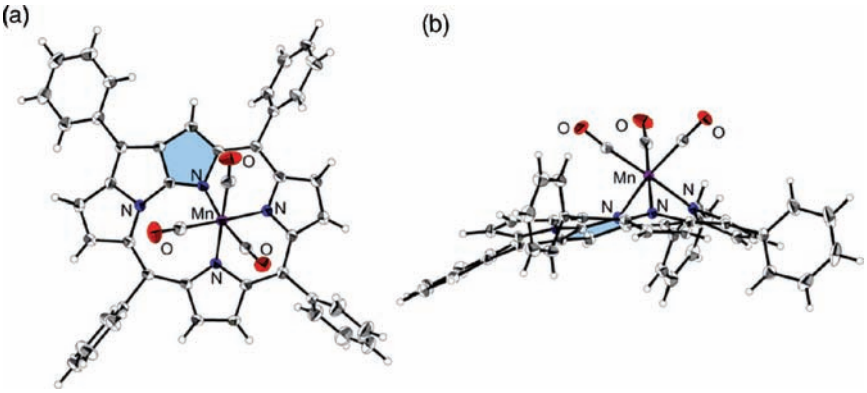

Figure 1. Crystal structure of **2a**; (a) top view, (b) side view. The solvent molecule is omitted for clarity. Thermal ellipsoids are shown at the 30% probability level.

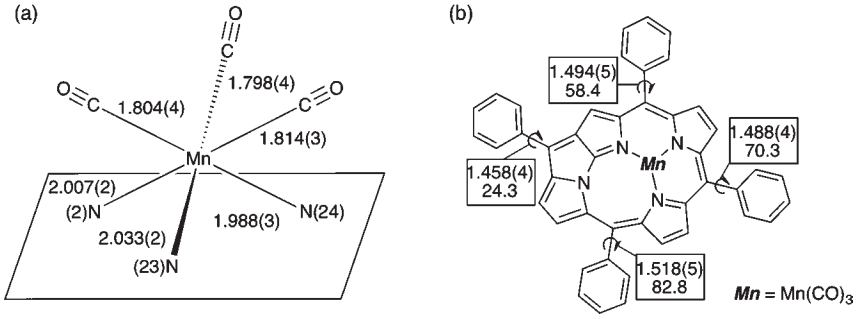

Figure 2. Structural details of **2a**; (a) the bond lengths (Å) around the metal center, (b) (upper) the bond lengths (Å) and (lower) the dihedral angles (deg) between the NFp plane and *meso*-phenyl rings.

dihedral angles of **2a** are shown in Figure 2. The three Mn−CO bond lengths (av 1.805 Å) are almost identical with those of $Mn(Tp')(CO)_3$ (av 1.809 Å) (Tp′: tetrakis(pyrazolyl)borate).[24] On the other hand, the three Mn−N bond lengths of **2a** (av 2.009 Å) are shorter than those of $Mn(Tp')(CO)_3$ (av 2.048 Å), implying strong bonding between the Mn ion and the NFp ligand. The dihedral angles between the NFp plane and the phenyl rings are 24.3° (5-phenyl), 82.8° (10-phenyl), 70.3° (15-phenyl), and 58.4° (20-phenyl). The 5-phenyl group is almost coplanar to the NFp plane, which enables the facile π-orbital interaction between the 5-phenyl group and the NFp π-system. As a result, the bond length between the C(5) *meso*-carbon atom and the phenyl ring (1.458(8) Å) is shorter than those of other phenyl groups (1.488(1)−1.517(8) Å). These structural features are similar to those of previously reported NFP free-base and metal complexes, indicating the rigidity of the NFp ligand.

Reaction of NFP Derivatives with $Mn(CO)_5Br$. To examine the effect of substituents on manganese(I) complexes, 21-substituted NFTPP derivatives, 21-bromo (**1b**), 21-nitro (**1c**), and 21-benzoyl (**1d**) were subjected to the reaction with $Mn(CO)_5Br$ in the presence of K_2CO_3 (Scheme 4). In the case of **1b**, the complexation proceeded smoothly to give the corresponding manganese(I) complex **2b** in 99% yield without a loss of bromo group. Meanwhile, the reactions of **1c** and **1d** with $Mn(CO)_5Br$ proceeded slowly and **2c** and **2d** were obtained in 18% and 46% yields, respectively, when the reaction was quenched after 30 min for comparison. The lower reactivity might be due to the electron-withdrawing groups at the 21-position,

Scheme 4. Reactions of 21-Substituted NFTPP with $Mn(CO)_5Br$

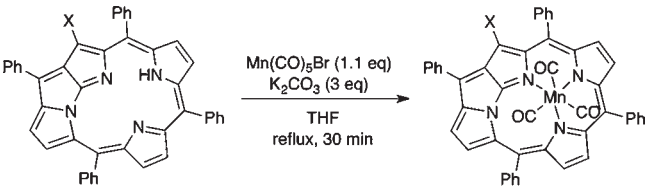

which decrease the basicity of the coordinating nitrogen atoms, hence the affinity to the metal center.

Chemical Modification of 2a. Peripheral modification of **2a** was achieved at the 21-position by the aromatic substitution reaction (Scheme 5). Nitration of **2a** with standard conditions ($NaNO_2$/HCl) proceeded instantly to afford 21-nitro derivative ($Mn^I(21\text{-}NO_2\text{-}NFTPp)(CO)_3$, **2c**) in 85% yield. The Vilsmeier−Haack formylation of **2a** with $POCl_3$/DMF gave 21-formyl derivative ($Mn^I(21\text{-}CHO\text{-}NFTPp)(CO)_3$, **2e**) in 93% yield. Similarly, chlorination of **2a** with N-chlorosuccinimide (NCS) afforded 21-chloro derivative ($Mn^I(21\text{-}Cl\text{-}NFTPp)(CO)_3$, **2f**) in 93% yield without a formation of di- or trichlorinated products. The regioselective aromatic substitution at the 21-position is one of the characteristic reactions of NFPs.[13,16b]

dx.doi.org/10.1021/ic2000393 |*Inorg. Chem.* 2011, 50, 6029–6043

Scheme 5. Regioselective Substitution Reactions of Manganese(I) NFTPP Complex (2a)

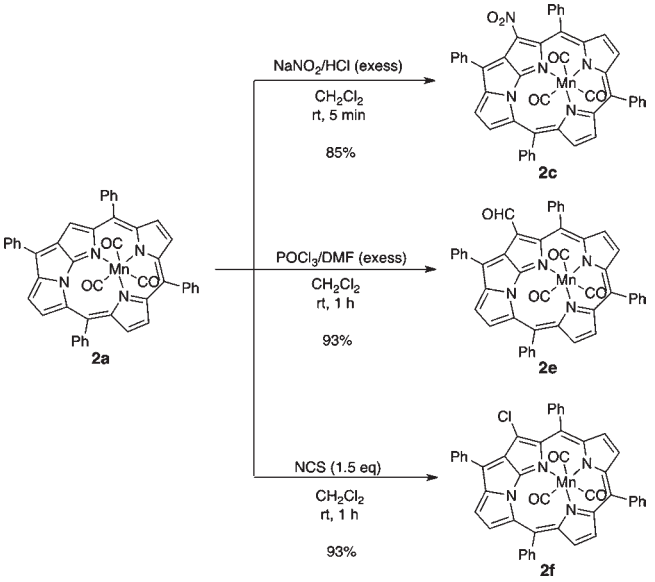

Metal-Assisted Transformation of 21-Substituted NCP to NFP Manganese(I) Complex. 21-Substituted NFP manganese(I) complexes (**2**) can be also prepared directly from the corresponding 21-substituted NCPs (**3**) and $Mn(CO)_5Br$ via skeleton rearrangement (Table 1). Upon heating a THF solution of 21-methyl NCTPP (**3g**)[25] with $Mn(CO)_5Br$ under basic conditions, the corresponding manganese(I) NFP complex (Mn^I(21-Me-NFTPp)$(CO)_3$, **2g**) was obtained in 43% yield (Entry 1). However, when the reaction was performed in toluene at reflux temperature, the yield was decreased abruptly (10%). Regardless the length of alkyl chains, the skeleton rearrangement from NCP to NFP proceeded smoothly to afford the corresponding complexes in similar yields (Entries 1−4). In the case of 21-benzyl NCTPP (**3k**), aside from the target NFP complex (Mn^I(21-Bn-NFTPp)-$(CO)_3$, **2k**) (11%), oxidized benzoyl derivatives, 21-Bz-NFTPP (**1d**) (21%), 21-Bz-NCTPP (**3d**) (19%), and Mn^I(21-Bz-NFTPp)$(CO)_3$ (**2d**) (2%), were also obtained.[26] On the other hand, in the case of electron-withdrawing substituents such as 21-nitro (**3c**)[27] and 21-chloro (**2f**) derivatives, the yields were low (**2c**: 10%, **2f**: 2%). In both cases, the electron-withdrawing groups were fallen off and the NCTPP-manganese(II) dimer complex (**5**) was obtained as a major product.[22a,c] Similarly, the reaction of parent NCTPP (**3a**) did not afford the NFP derivative instead the dimer complex **5** was obtained (Scheme 2b). Thus, the bulky substituents at the 21-position may play an important role for such transformation. In the solid state, the confused pyrrole ring of **3c** is largely tilted by 42.4° from the porphyrin mean plane compared to that of **3a**, 26.9°.[3b,4a,28] Thus, the introduction of a bulky group to the inner C(21) atom of **3a** would cause a large inclination of the confused pyrrole, which may facilitate the ring rotation necessary for the ring-fusion. It may also affect as a steric hindrance that suppresses the dimerization reaction. Alternately, when a THF solution of 21-substituted NCTPP (**3**) was refluxed in the absence of $Mn(CO)_5Br$, no reaction took place, which further supports the necessary requirement of manganese center for facile conversion of NCP to NFP.

Table 1. Reactions of 21-Substituted NCTPP (3) with $Mn(CO)_5Br$

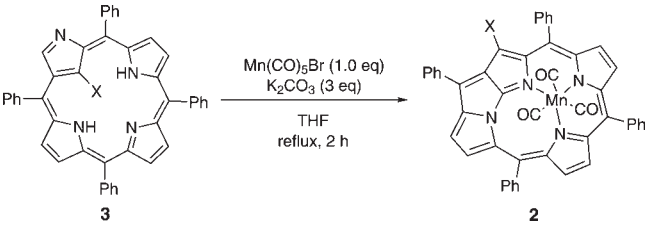

entry	NCP	−X	NFP	yield (%)
1	**3g**	$-CH_3$	**2g**	43
2	**3h**	$-CH_2CH_2CH_3$	**2h**	40
3	**3i**	$-CH_2CH(CH_3)_2$	**2i**	40
4	**3j**	$-CH(CH_3)_2$	**2j**	42
5	**3k**	$-CH_2Ph$	**2k**	11
6	**3c**	$-NO_2$	**2c**	10
7	**3f**	−Cl	**2f**	2
8	**3a**	−H	**2a**	0

Concerning the structures of 21-substituted manganese(I) complexes (**2**), X-ray single crystallographic analyses were performed on **2h** and **2i** (Figure 3). The averaged bond lengths (Å) of Mn−CO and Mn−N of **2h** (1.799(6), 2.003(4)) and **2i** (1.793(3), 1.994(2)) are shorter than those of **2a** (1.805(4), 2.009(2)), indicating the stronger binding between the manganese(I) ion and the NFp ligands (Figure 4). The electron-donating property of the alkyl groups may increase the basicity of the nitrogen atoms, and hence the affinity to the metal center.

To understand the reaction mechanism that is reasonable for the formation of either NCP-manganese(II) dimer complex (**5**) or NFP-manganese(I) monomer complex (**2**), the reaction mixture was subjected for the mass analysis. During the course of reactions, initial formation of NCP-manganese species was clearly observed. For example, the molecular ion peaks corresponding to 21-isobutyl NCTPP-manganese complex (m/z = 723 and 724; no peak was detected at m/z = 722) were detected in the MALDI-TOF mass spectrum of the reaction mixture of 21-^{i}Bu-NCTPP (**3i**) with $Mn(CO)_5Br$. Although the valency of the manganese ion could not be explicitly determined from the mass spectra, it is highly probable that the coordination of manganese(I) to 21-substituted NCTPP (**3**) took place first with release of a HBr molecule, then afforded the NFP manganese(I) complex (**2**) via ring rearrangement (Scheme 6). In the case of intact NCP (**3a**), however, the oxidation of the metal center, probably by the NCP ligand, could proceed after the initial complexation, then followed by the release of both the CO ligands and the outer NH proton to afford the NCP-manganese(II) complex (**5**) (Scheme 6, path-a). Such an electron and proton transfer coupled reaction is one of the characteristics of the NCP ligand, as illustrated in the nitrite reduction with the iron(II) NCP complex by Hung and co-workers.[29] In the presence of the electron-donating alkyl groups, the oxidation of the metal center by the NCP ligand would be largely deterred; as a result, the formation of **5**, may be suppressed and consequently, the reaction pathway to the NFP manganese complexes (**2**) via ring rotation would become predominant (Scheme 6, path-b).

dx.doi.org/10.1021/ic2000393 |*Inorg. Chem.* 2011, 50, 6029–6043

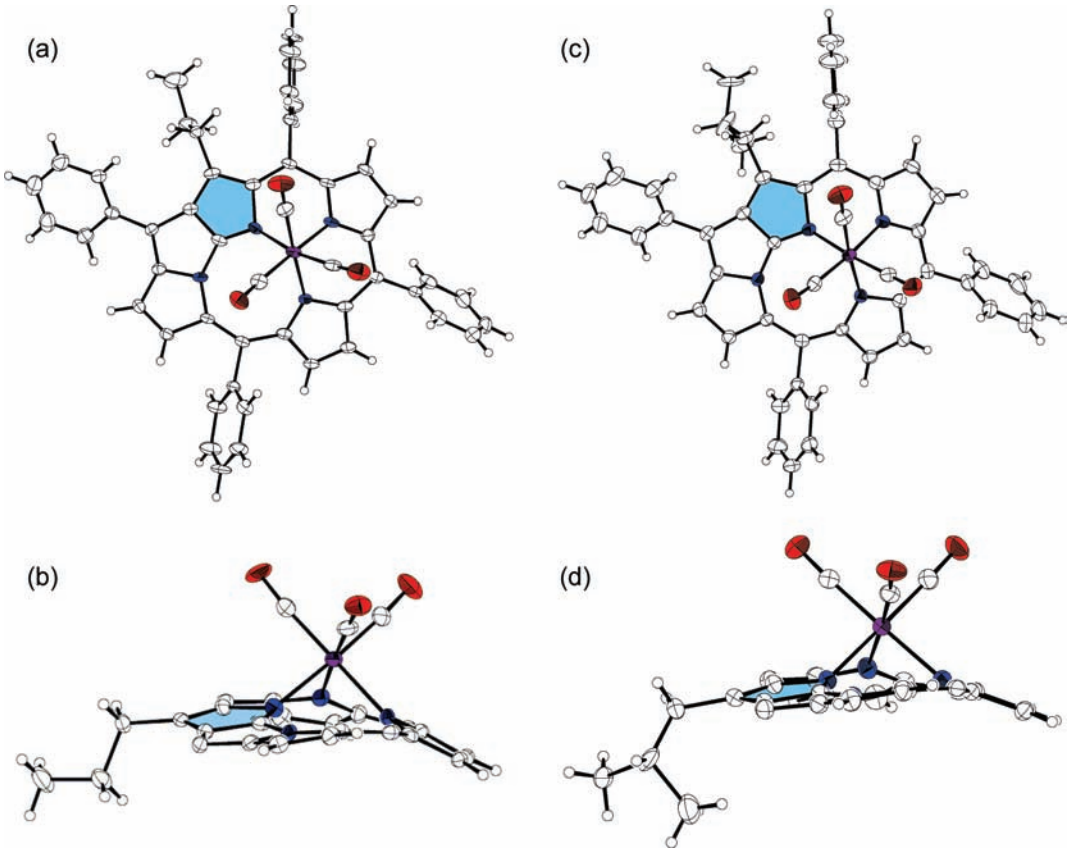

Figure 3. Crystal structures of 21-propyl and 21-isobutyl NFTPP manganese(I) complexes (**2h**, **2i**); (a) top view of **2h**, (b) side view of **2h**, (c) top view of **2i**, (d) side view of **2i**. *Meso*-phenyl groups are omitted for clarity in the side views. Thermal ellipsoids are shown at the 30% probability level.

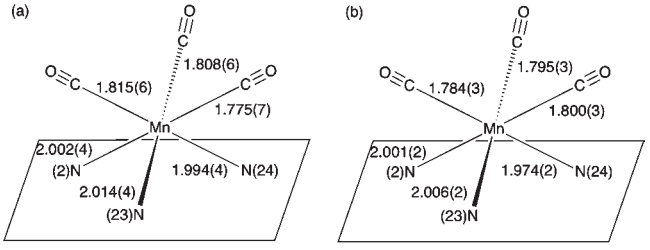

Figure 4. Bond lengths (Å) around the metal center of 21-alkyl NFTPP manganese(I) complexes; (a) **2h**, (b) **2i**.

UV−vis−NIR Absorption. The absorption spectra of manganese(I) NFP complexes **2** were measured in CH_2Cl_2. The numerical data are summarized in Table 2, and the corresponding spectra of **2a**, **2c**, and **2g** are shown in Figure 5. In the absorption spectrum of **2a**, the Soret-like bands were observed at 352 and 497 nm, and Q-like bands at 848 and 942 nm. The absorption spectrum of **2a** is quite similar to that of **1a** with the absorption edge reaching to 1000 nm, indicating that the manganese coordination does not alter the aromaticity of the NFP skeleton. The effect of 21-substituents on the Q- and Soret-like bands was examined using **2a** as a standard. For the electron-withdrawing groups, Q-like bands are blue-shifted (Entries 7−9), whereas for the electron-donating groups, red-shifts are induced (Entries 2−6). On the other hand, the Soret-like bands are red-shifted for the electron-withdrawing groups (Entries 7−9) and blue-shifted for the electron-donating groups (Entries 2−6). Introduction of halogen groups caused the red-shifts for Q-like bands (Entries 11−12). The observed effects of substituent on the absorption spectra of **2** are similar to those of free-base NFP derivatives, which suggests the metal−ligand charge-transfer (MLCT) nature is negligible in the electronic absorption of the manganese(I) NFP complexes (**2**).

Electrochemical Measurements. Cyclic voltammetry measurements on the NFP manganese(I) complexes (**2**) revealed that they are robust under the electrochemical conditions, allowing the complexes to be oxidized and reduced without a loss of manganese center. As a typical example, the cyclic voltammogram of **2a** is shown in Figure 6, and the electrochemical data for a series of manganese(I) NFP complexes (**2a**−**k**) are summarized in Table 3. In a CH_2Cl_2 solution of **2a**, a reversible one-electron oxidation peak at 0.34 V and two reversible one-electron reduction peaks at −1.32 and −1.76 V (vs Fc/Fc^+) were observed, respectively. As compared to **2a** (Entry 1), the oxidation potentials are negatively shifted for the complexes with electron-donating groups (Entries 2−6) and positively shifted in the presence of electron-withdrawing groups (Entries 7−11). A similar trend was apparently observed for the reduction potentials. Nevertheless, no significant differences are observed in the $E_{Ox1}-E_{Red1}$ value that directly correlates with the HOMO−LUMO energy gap. These redox potentials are similar to those of the parent NFTPP derivatives (E_{Ox1}: 0.16 V (irreversible), E_{Red1}: −1.39 V (reversible) for NFTPP),[16] but slight positive shifts were observed. In addition, a negligible contribution of the Mn atom was observed in both HOMO and LUMO of **2a** (vide infra). Accordingly, the observed oxidation

dx.doi.org/10.1021/ic2000393 |*Inorg. Chem.* 2011, 50, 6029–6043

Scheme 6. Plausible Reaction Pathways of NCTPP Derivatives with Manganese Reagent

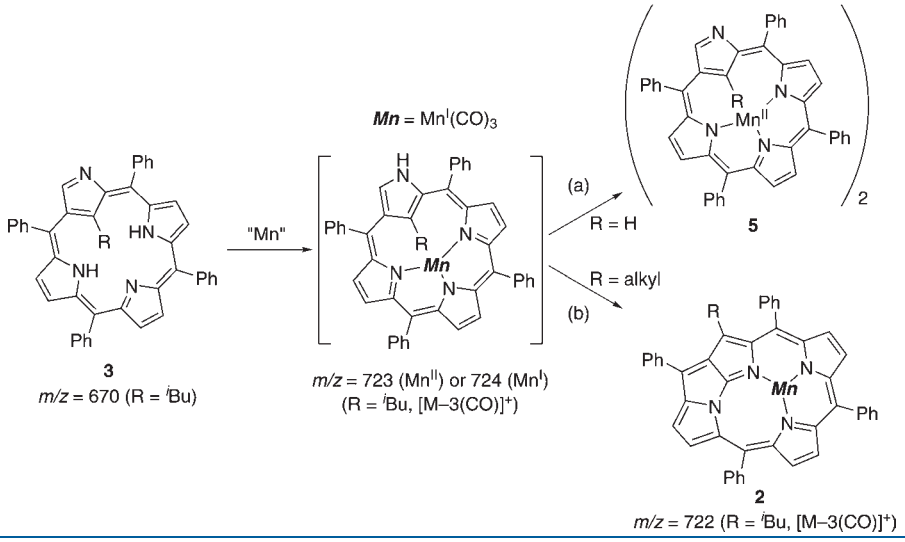

Table 2. Absorption Spectral Data for the NFP Manganese(I) Complexes (2) in CH_2Cl_2

entry	NFP	–X	λ_{max} (nm) (log ε)				
1	**2a**	–H	352 (4.76)	497 (4.84)		848 (3.49)	942 (3.46)
2	**2g**	$-CH_3$	348 (4.53)	493 (4.55)		873 (3.26)	963 (3.19)
3	**2h**	$-CH_2CH_2CH_3$	348 (4.43)	492 (4.47)		867 (3.15)	961 (3.11)
4	**2i**	$-CH_2CH(CH_3)_2$	348 (4.30)	493 (4.33)		869 (3.09)	960 (2.99)
5	**2j**	$-CH(CH_3)_2$	346 (4.63)	488 (4.64)		861 (3.30)	952 (3.27)
6	**2k**	$-CH_2Ph$	348 (4.52)	493 (4.57)		858 (3.25)	953 (3.20)
7	**2c**	$-NO_2$	357 (4.51)	515 (4.69)	679 (3.79)	772 (3.50)	862 (3.25)
8	**2e**	–CHO	355 (4.42)	508 (4.59)		799 (3.31)	879 (3.24)
9	**2d**	–COPh	356 (4.35)	502 (4.47)		828 (3.15)	908 (3.09)
11	**2b**	–Br	352 (4.57)	496 (4.64)	651 (3.74)	858 (3.33)	954 (3.27)
12	**2f**	–Cl	353 (4.40)	497 (4.46)		872 (3.13)	959 (3.07)

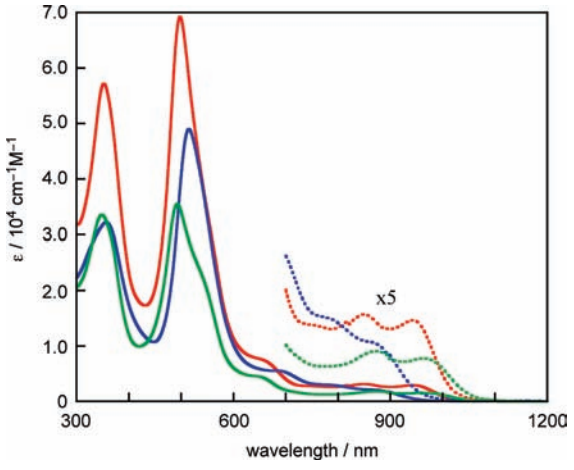

Figure 5. Absorption spectra of **2a** (red), **2c** (blue), and **2g** (green) in CH_2Cl_2.

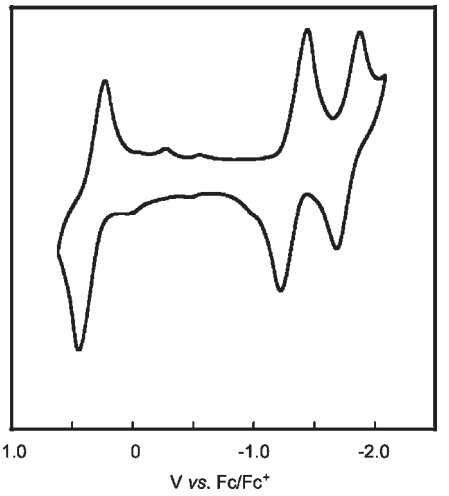

Figure 6. Cyclic voltammogram of **2a** in CH_2Cl_2 with 0.1 M Bu_4NPF_6 (Pt electrode, scan rate 100 mV/s).

and reduction of NFTPP manganese tricarbonyl complexes would not occur at the metal center but at the NFP skeletons.

Molecular Orbital. The Kohn–Sham orbitals of **2a** calculated at the B3LYP/631T level are shown in Figure 7.[30] Both the HOMO and LUMO are distributed over the NFTPp skeleton, and reflecting the coplanarity of the NFP core, a contribution from the 5-phenyl group is also observed in the HOMO. In the

dx.doi.org/10.1021/ic2000393 |Inorg. Chem. 2011, 50, 6029–6043

Table 3. Formal Potentials (V vs Fc/Fc^+) of Manganese(I) NFP Complexes (2) in CH_2Cl_2 Containing 0.1 M Bu_4NPF_6

entry	NFP	−X	E_{Ox1}	E_{Red1}	E_{Red2}	$E_{Ox1} - E_{Red1}$
1	**2a**	−H	0.34	−1.32	−1.76	1.68
2	**2g**	$-CH_3$	0.24	−1.40	−1.80	1.64
3	**2h**	$-CH_2CH_2CH_3$	0.28	−1.36	−1.80	1.64
4	**2i**	$-CHCH_2(CH_3)_2$	0.25	−1.41	−1.86	1.66
5	**2j**	$-CH(CH_3)_2$	0.28	−1.42	−1.85	1.70
6	**2k**	$-CH_2Ph$	0.29	−1.38	−1.83	1.67
7	**2c**	$-NO_2$	0.66	−1.05	−1.43	1.71
8	**2e**	−CHO	0.52	−1.15	−1.54	1.67
9	**2d**	−COPh	0.42	−1.25	−1.67	1.67
10	**2b**	−Br	0.37	−1.25	−1.66	1.62
11	**2f**	−Cl	0.35	−1.27	−1.68	1.62

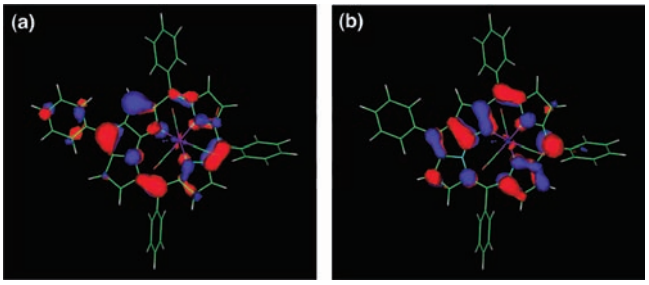

Figure 7. Kohn−Sham orbitals of **2a**; (a) HOMO, (b) LUMO.

both orbitals, negligible contribution from the manganese metal is observed, which suggests the first electrochemical redox process of **2a** occurs at the NFTPp moiety similar to the rhenium complex **4a**.[16b]

Protonation of Mn^I(NFTPp)$(CO)_3$ (2a). Addition of acids to **2a** caused protonation, and no decomposition or demetalation was observed. For example, when an excess amount of methanesulfonic acid (MSA) was added to a CH_2Cl_2 solution of **2a**, the color changed instantly from purple-red to brown, and the original purple-red color was regenerated by the subsequent treatment with Et_3N. The ^1H NMR spectra of **2a** with/without MSA in $CDCl_3$ are shown in Figure 8. In the presence of MSA, the signals around the aromatic region, which appear between 7.4−9.4 ppm in the free-base, shifted to a lower-field and appeared between 7.6−10.2 ppm. In addition, one new broad signal was observed at −1.04 ppm at 233 K, which suggests that the protonation occurs inside of the aromatic NFP core. The site of protonation could not be explicitly determined, but it is most likely to take place at the nitrogen atom and not at the carbon atom (C3) because no corresponding cross peak was observed in the $^1H-^{13}C$ heteronuclear multiple quantum coherence (HMQC),[31] NOE, and H−H COSY measurements and a large relative energy for the C(3)-protonated species was inferred from the calculation study (vide infra). Interestingly, when the trifluoroacetic acid (TFA) was added, a different behavior was observed in the ^1H NMR spectra. Namely, in addition to the previously observed species, a small amount of a C(21)-protonated one (the ratio was ca. 3:1 based on the ^1H NMR signals) was newly formed, judging from the appearance of two doublet signals at 4.86 and 5.25 ppm with a large coupling constant $^2J_{(H,H)}$ = 24.4 Hz, which are attributable to the CH_2 group at the

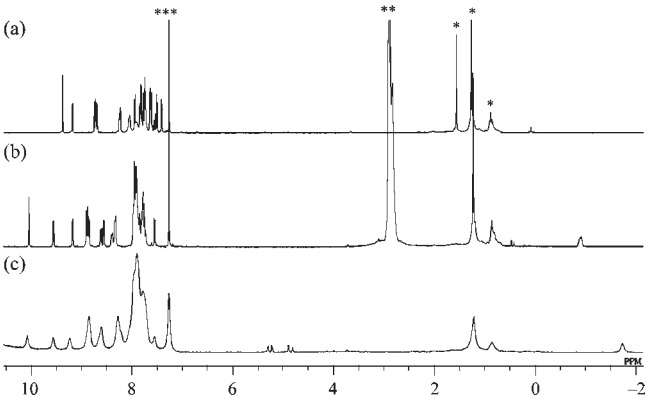

Figure 8. ^1H NMR spectra of (a) **2a** at ambient temperature, (b) **2a** + MSA at 233 K, and (c) **2a** + TFA, at 233 K in $CDCl_3$. *, impurity; **, MSA; ***, solvent.

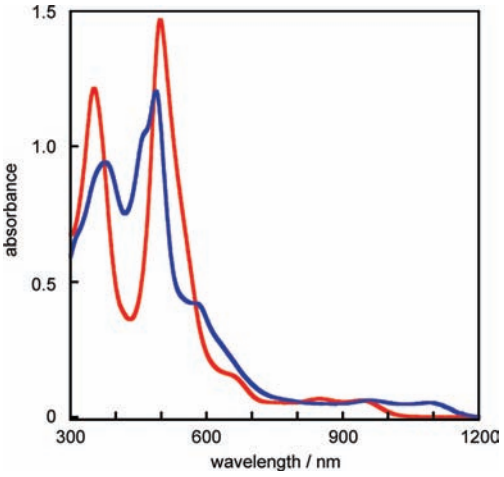

Figure 9. Absorption spectra of **2a** (red) and **2a** + MSA (blue) in CH_2Cl_2.

21-position. Such protonation was previously observed in the rhenium(I) NFP complex (**4a**).[16b] In the IR spectra of **2a** with MSA, 1−3 cm^{-1} shifts of CO stretching were observed: 2005 (2007), 1920 (1921), 1902 (1905) cm^{-1}, which may also support the protonation at the nitrogen atom, though the shifts are modest. In the absorption spectrum of **2a** with MSA, the Soret-like bands were observed at 377 and 489 nm, and a Q-like band was observed at 1094 nm. In contrast to the small blue-shift (ca. 8 nm) of the former electronic transition, a significant red-shift (150 nm) was observed for the Q-like band upon protonation (Figure 9).

To find the appropriate site of protonation on the NFP complex, we have carried out the density functional theory (DFT) calculations on the possible isomers of protonated **2a**. The relative energies, HOMO−LUMO energies, and the calculated ^1H NMR chemical shifts of the added proton in protonated species (**2aP-1**−**2aP-8**) are shown in Figure 10. Among the 8 isomers considered, **2aP-6** is the most stable and **2aP-3** is the second most stable with the energy difference of 1.67 kcal/mol. Thus, based on the calculations, the protonated species in the solution is presumed to be **2aP-6**. The two species observed in the case of TFA addition could be assigned as **2aP-6** (major) and

dx.doi.org/10.1021/ic2000393 |*Inorg. Chem.* 2011, 50, 6029–6043

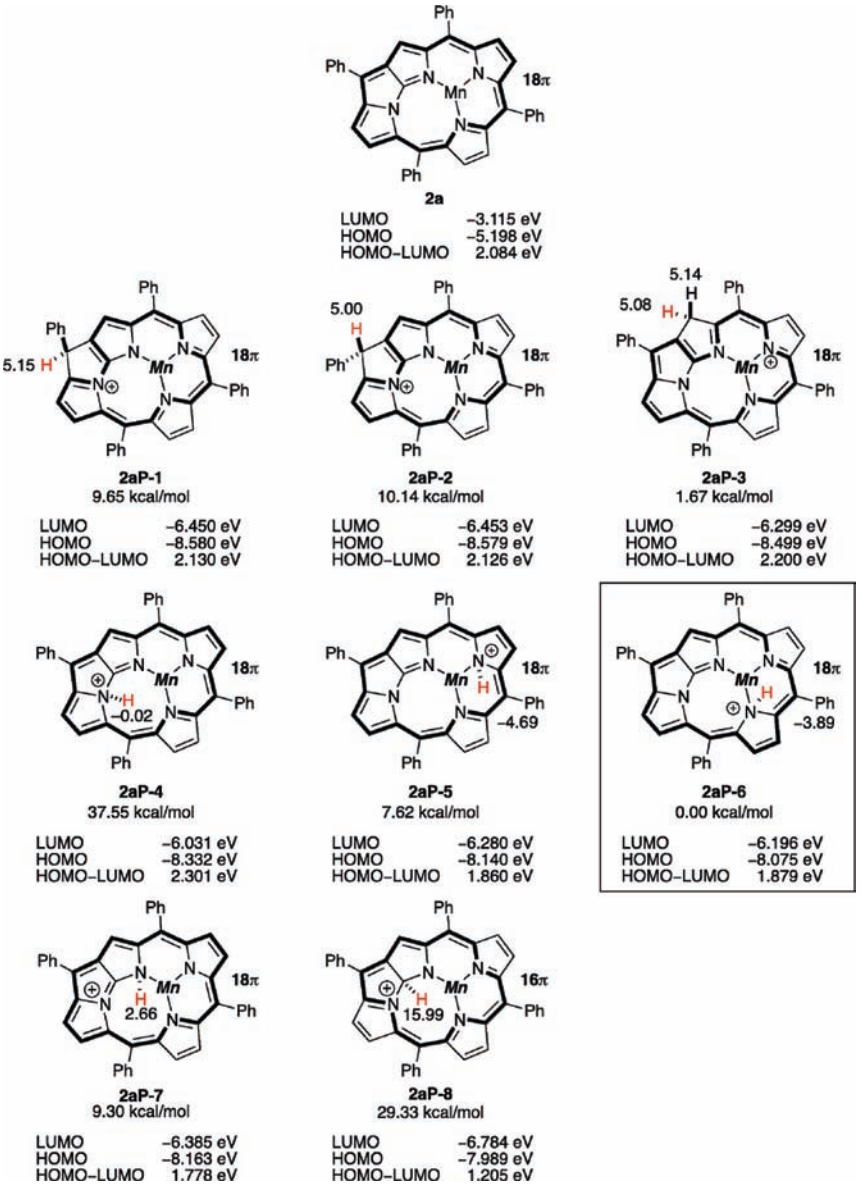

Figure 10. Relative energies, calculated ^{1}H NMR chemical shifts (ppm) of the acid proton (red), and the HOMO−LUMO energies of **2a** and protonated species (**2aP-1**−**2aP-8**).

2aP-3 (minor). The possibility of *C*-protonation at the C(3)-position (**2aP-8**) could be excluded because **2aP-8** possesses a high relative energy (29.33 kcal/mol) with a 16π antiaromatic character. The calculated HOMO−LUMO gap energy of **2aP-6** is smaller than that of **2a**, which is consistent with the bathochromic shift of the Q-like band. Although no clear proof is provided, it is likely that the relative energies of the protonated species are largely influenced by the conjugate bases present in the solution.[32]

Oxidative-Demetalation. The manganese metal in **2** can be removed by the oxidation with amine *N*-oxides. When the complex **2a** was treated with 9 equiv of $Me_3NO\cdot 2H_2O$ in toluene under reflux conditions for 30 min, demetalation occurred to give the free-base **1a** in 85% yield (Scheme 7). On the other hand, when the reaction was performed with a stoichiometric amount of $Me_3NO\cdot 2H_2O$, no demetalated species were observed on thin layer chromatography (TLC) as

Scheme 7. Oxidative Demetalation Reaction of NFP-Manganese(I) Complexes (2)

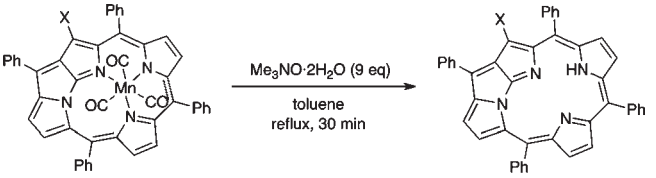

2a: X = H
2c: X = NO_2
2g: X = CH_3

1a: 85%
1c: 51%
1g: 68%

well as in the ^{1}H NMR analysis. The reaction of **2a** with *N*-methylmorpholine *N*-oxide also proceeded to give **1a**, whereas the reaction with *t*-BuOOH resulted in the formation of highly polar unknown fractions but not **1a**. Thus, the usage of amine

dx.doi.org/10.1021/ic2000393 |*Inorg. Chem.* 2011, 50, 6029–6043

N-oxide reagents as oxidant seems so far important for demetalation of **2a**. Similarly, the 21-substituted NFP manganese(I) complexes (**2g**, **2c**) were demetalated by $Me_3NO \cdot 2H_2O$ to afford **1g** and **1c** in 68 and 52% yield, respectively. Though the specific role of amine *N*-oxide is not clear, it might be related to its ability to oxidize CO ligands selectively to carbon dioxides.[33] Using this oxidative-demetalation reaction, free-base forms of 21-substituted NFP and other related compounds could be prepared easily.

Comparison of Manganese and Rhenium NFP Complexes. The similarity and difference between the manganese(I) and rhenium(I) complexes, $Mn^{I}(NFTPp)(CO)_3$ (**2a**) and $Re^{I}(NFTPp)(CO)_3$ (**4a**), respectively, are summarized. At first, both metal complexes can be readily synthesized from the reaction of NFP and the corresponding metal reagents in good yields. The reaction of NCTPP (**3a**) with manganese reagents affords NCP-manganese(II) dimer **5**; on the other hand, with the rhenium reagent, NFP-rhenium(I) complex **4a** is obtained.[16b] The reaction of 21-Me-NCTPP (**3g**) with $Mn(CO)_5Br$ affords the Mn^{I}(21-Me-NFTPp)$(CO)_3$ (**2g**), while the reaction of **3g** with $Re_2(CO)_{10}$ afforded a peculiar [5.6.5]-fused NCP rhenium(I) tricarbonyl complex possessing an *N*-heterocyclic carbene moiety.[34] The facile formation of manganese(II) NCP dimer species could be relevant to the weaker binding of the CO ligands to the manganese metal center compared to the rhenium.[35] The redox potentials of manganese(I) NFP complex **2a** (0.34, −1.32 V) are more negatively shifted than those of rhenium(I) NFP complex **4a** (0.47, −1.21 V), which could be attributed to the lower electronegativity of Mn (1.55) than Re (1.90).[36] In the absorption spectra, both complexes show a similar trend with the Soret and Q-like bands although the absorption maximum at the longest wavelength is more hypsochromic shifted for **2a** (Mn: 942 nm, Re: 951 nm). Protonation on manganese(I) NFP complex **2a** using MSA takes place at the N(23)-position (**2aP-6**), and the protonation with TFA affords a mixture of *N*-protonation (**2aP-6**) and *C*-protonation (**2aP-3**). On the other hand, in the case of the rhenium(I) NFP complex **4a**, protonation with TFA occurs selectively at the C(21)-position to afford **2aP-3** type species.[32] The decrease of *N*-protonation in the rhenium(I) NFP complex **4a** could be explained by the lower basicity of the coordinating nitrogen atoms compared to that of **2a**. Because of the higher electronegativity of rhenium than manganese, electron density of the coordinating nitrogen atoms of **4a** would become lower than that of manganese(I) complex **2a**, which may result in lowering the basicity of the nitrogen atoms, and hence lower the proton affinity. On treatment with amine *N*-oxides, the rhenium(I) NFP complex **4a** is oxidized to rhenium(VII) species, $Re^{VII}(NFTPp)O_3$,[17,18] whereas the manganese complex **2a** is demetalated to afford free-base **1a**.

CONCLUSION

A series of manganese(I) tricarbonyl complexes of N-fused tetraphenylporphyrin and its 21-substituted derivatives (**2**) were successfully prepared, and their optical and electrochemical properties and reactivity were investigated. The NFP manganese complexes (**2**) can be prepared from N-fused porphyrins (**1**) with $Mn(CO)_5Br$ as well as directly from the 21-substituted N-confused porphyrins (**3**) via metal-induced ring rearrangement reactions. Regioselective aromatic substitution reactions of **2** occurred at the C(21)-position without a loss of metal center. In the electrochemical measurements for **2**, one reversible oxidation wave and two reversible reduction waves are observed. Their redox potentials implied narrow HOMO−LUMO gaps of **2** and are consistent with their absorption spectra, in which the absorption edges exceed 1000 nm. On treatment with amine *N*-oxides, demetalation of **2** proceeded to afford the corresponding NFP free-bases (**1**). Such features would enable us to access the novel NFP derivatives as well as NFP metal complexes of the other 3d-transition metals that could exhibit unusual properties different from those of porphyrin complexes.[37] Further study on the N-fused porphyrin metal complexes is now underway.

EXPERIMENTAL SECTION

General Procedures. Commercially available solvents and reagents were used without further purification. N-confused porphyrins and N-fused porphyrins were obtained by methods already described.[3,25,27,38] Thin layer chromatography (TLC) was carried out on aluminum sheets coated with silica gel 60 (Merck 5554). Preparative purifications were performed by flash column chromatography (KANTO Silica Gel 60 N, spherical, neutral, 40−50 μm), and gravity column chromatography (KANTO Silica Gel 60 N, spherical, neutral, 63−210 μm). The ^{1}H NMR spectra were recorded on a JNM-AI SERIES FT-NMR spectrometer (JEOL) at 300 MHz. Proton chemical shifts were reported relative to the residual proton of the deuterated solvent (δ = 7.26 ppm for $CHCl_3$). ^{13}C NMR spectra were recorded at 75 MHz, and chemical shifts were reported relative to $CDCl_3$ (δ = 77.00) in ppm. UV−vis−NIR absorption spectra were recorded on an UV-3150PC spectrometer (Shimadzu). Mass spectra were recorded on a Bruker Daltonics autoflex MALDI-TOF MS spectrometer and a JEOL JMS-T100CS (ESI mode). Cyclic voltammetric measurements were performed on a CH Instrument Model 620B (ALS) equipped with a Pt electrode. All the measurements were achieved in 0.1 M Bu_4NPF_6 solution of CH_2Cl_2 (deoxygenated by Ar bubbling over 30 min) with a scan rate of 100 mV/s under Ar atmosphere. A Ag/Ag+ electrode was used for the reference electrode and freshly sublimed ferrocene was used as external standard to determine redox potentials. IR absorption spectra were recorded on FT/IR-4200 (JASCO).

Reactions of N-Fused Tetraphenylporphyrins with $Mn(CO)_5Br$. *Manganese(I) N-Fused Tetraphenylporphyrinato Tricarbonyl Complex (Mn^{I}(NFTPp)$(CO)_3$, **2a**) (Typical Procedure).* A solution of NFTPP (**1a**) (120 mg, 200 μmol, 1.0 equiv), $Mn(CO)_5Br$ (59.4 mg, 220 μmol, 1.1 equiv), and K_2CO_3 (82.8 mg, 600 μmol, 3.0 equiv) in THF (15 mL) was refluxed for 30 min. After cooling, the solvent was removed under reduced pressure, and the residue was purified by silica gel column chromatography (eluent: CH_2Cl_2/hexane = 2/1). The first reddish purple fraction was collected and concentrated to dryness to give **2a** in 88% yield (133 mg, 177 μmol).

^{1}H NMR ($CDCl_3$, 300 MHz, ppm): δ 7.42 (d, J = 4.4 Hz, 1H), 7.51 (d, J = 4.9 Hz, 1H), 7.52−7.54 (m, 1H), 7.60 (d, J = 4.4 Hz, 1H), 7.62−7.65 (m, 3H), 7.72−7.85 (m, 8H), 7.90−7.92 (m, 2H), 7.93 (d, J = 4.9 Hz, 1H), 8.05−8.08 (m, 2H), 8.24−8.27 (m, 2H), 8.68 (d, J = 4.9 Hz, 1H), 8.72 (d, J = 7.3 Hz, 2H), 9.18 (d, J = 4.9 Hz, 1H), 9.36 (s, 1H); ^{13}C NMR ($CDCl_3$, 75 MHz, ppm): δ 111.79, 112.04, 118.88, 120.59, 125.37, 127.18, 127.37, 127.46, 127.52, 128.01, 128.08, 128.20, 128.44, 129.16, 129.29, 129.75, 130.37, 130.67, 132.35, 133.11, 133.38, 135.22, 135.35, 135.75, 138.05, 138.57, 138.61, 142.98, 145.44, 149.19, 153.94, 154.31, 154.77, 159.11, 165.12, 214.08, 216.33, 216.82; MS (MALDI, positive): m/z 666.16 ($[M-3CO]^+$); HRMS (ESI^+): Found: m/z 751.15155, Calcd for $C_{47}H_{28}MnN_4O_3(MH^+)$: m/z 751.15419; Anal. Calcd for **2a** $\cdot CH_2Cl_2$ ($C_{48}H_{29}Cl_2MnN_4O_3$): C, 68.99; H, 3.50; N, 6.70. Found: C, 69.09; H, 3.76; N, 6.57; UV−vis−NIR (CH_2Cl_2, λ_{max}/nm, (log ε)): 942 (3.46), 848 (3.49), 497 (4.84), 352 (4.76); IR (powder, cm^{-1}, CO): 1902, 1920, 2005.

2a + MSA. ^{1}H NMR ($CDCl_3$, 300 MHz, 233 K, ppm): δ −1.04 (s, 1H), 7.55 (d, J = 4.3 Hz, 1H), 7.75−7.82 (m, 4H), 7.84−7.98 (m, 11H), 8.31−8.33 (m, 2H), 8.36−8.41 (m, 1H), 8.56 (d, J = 4.5 Hz, 1H), 8.60−8.63 (m, 1H), 8.85 (d, J = 4.9 Hz, 1H), 8.88−8.91 (m, 2H), 9.20 (d, J = 4.5 Hz, 1H), 9.57 (d, J = 4.9 Hz, 1H), 10.07 (s, 1H); ^{13}C NMR ($CDCl_3$, 75 MHz, ppm): δ 116.33, 117.37, 123.08, 125.16, 126.97, 128.20, 128.37, 129.01, 129.43, 130.04, 130.14, 130.44, 130.65, 130.99, 131.73, 132.05, 132.38, 133.02, 133.23, 133.66, 134.45, 134.84, 135.13, 135.96, 136.53, 138.54, 140.85, 142.86, 145.97, 150.11, 152.62, 154.34, 157.58, 158.46, 158.79, 211.77, 213.24, 216.24; IR (powder, cm^{-1}, CO): 1905, 1921, 2007.

Manganese(I) 21-Bromo N-Fused Tetraphenylporphyrinato Tricarbonyl Complex (Mn^I(21-Br-NFTPp)(CO)$_3$, ***2b****).* Starting from 21-Br-NFTPP (**1b**) (31.0 mg, 45 μmol, 1.0 equiv), **2b** was obtained in 99% yield (36.5 mg, 44 μmol). ^{1}H NMR ($CDCl_3$, 300 MHz, ppm): δ 7.45 (d, J = 4.6 Hz, 1H), 7.53 (d, J = 4.9 Hz, 1H), 7.57−7.62 (m, 2H), 7.66−7.68 (m, 4H), 7.73−7.78 (m, 9H), 7.94−7.96 (m, 2H), 7.97 (d, J = 4.9 Hz, 1H), 8.06−8.09 (m, 2H), 8.51−8.53 (m, 2H), 8.71 (d, J = 5.2 Hz, 1H), 9.04 (d, J = 5.2 Hz, 1H); ^{13}C NMR ($CDCl_3$, 75 MHz, ppm): δ 98.63, 112.51, 118.90, 120.83, 125.11, 126.42, 127.36, 127.46, 127.54, 127.98, 128.10, 128.33, 128.80, 129.04, 130.94, 131.20, 132.50, 132.98, 133.08, 133.55, 136.03, 136.13, 136.47, 138.37, 139.15, 142.55, 144.02, 145.21, 154.55, 154.66, 157.90, 165.71, 213.91, 216.62, 216.84; MS (MALDI, positive): m/z 745.16 ([M-3CO]$^+$), 665.43 ([M-3CO-Br]$^+$); HRMS (ESI$^+$): Found: m/z 828.05602, Calcd for $C_{47}H_{26}MnBrN_4O_3$(M^+): m/z 828.05688; Anal. Calcd for **2b**·0.1CH_2Cl_2 ($C_{47.1}H_{26.2}BrCl_{0.2}MnN_4O_3$): C, 67.50; H, 3.15; N, 6.69. Found: C, 67.59; H, 3.36; N, 6.43; UV−vis−NIR (CH_2Cl_2, λ_{max}/nm, (log ε)): 954 (3.27), 858 (3.33), 651 (3.74), 496 (4.64), 352 (4.57); IR (powder, cm^{-1}, CO): 1904, 1915, 2005.

Manganese(I) 21-Nitro N-Fused Tetraphenylporphyrinato Tricarbonyl Complex (Mn^I(21-NO$_2$-NFTPp)(CO)$_3$, ***2c****).* Starting from 21-NO$_2$-NFTPP (**1c**) (30.4 mg, 46 μmol, 1.0 equiv), **2c** was obtained in 18% yield (6.6 mg, 8 μmol). ^{1}H NMR ($CDCl_3$, 300 MHz, ppm): δ 7.56 (d, J = 4.6 Hz, 1H), 7.60−7.62 (m, 1H), 7.65−7.73 (m, 9H), 7.75−7.95 (m, 6H), 7.94−7.96 (m, 2H), 8.09 (d, J = 7.9 Hz, 2H), 8.19 (m, 3H), 8.89 (d, J = 5.0 Hz, 1H), 9.13 (d, J = 5.0 Hz, 1H); ^{13}C NMR ($CDCl_3$, 75 MHz, ppm): δ 113.91, 119.99, 121.55, 121.70, 126.74, 127.35, 127.65, 128.08, 128.54, 128.56, 128.65, 128.80, 129.25, 130.56, 130.90, 130.93, 131.81, 132.40, 132.50, 132.78, 133.51, 135.44, 135.48, 137.03, 137.64, 137.77, 137.99, 139.42, 144.84, 146.32, 155.31, 156.19, 157.04, 157.32, 165.05, 167.79, 213.26, 214.65, 215.58; MS (MALDI, positive): m/z 711.01 ([M−3CO]$^+$); HRMS (ESI$^+$): Found: m/z 796.14126, Calcd for $C_{47}H_{27}MnN_5O_5$(MH^+): m/z 796.13927; Anal. Calcd for **2c**·0.7CH_2Cl_2 ($C_{47.7}H_{27.4}Cl_{1.4}MnN_5O_5$): C, 67.00; H, 3.23; N, 8.19. Found: C, 66.78; H, 3.43; N, 8.36; UV−vis−NIR (CH_2Cl_2, λ_{max}/nm, (log ε)): 862 (3.25), 772 (3.50), 679 (3.79), 515(4.69), 357 (4.51); IR (powder, cm^{-1}, CO): 1896, 1916, 2006.

Manganese(I) 21-Benzoyl N-Fused Tetraphenylporphyrinato Tricarbonyl Complex (Mn^I(21-Bz-NFTPp)(CO)$_3$, ***2d****).* Starting from 21-Bz-NFTPP (**1d**) (16.6 mg, 23 μmol, 1.0 equiv), **2d** was obtained in 46% yield (8.9 mg, 11 μmol). ^{1}H NMR ($CDCl_3$, 300 MHz, ppm): δ 7.15−7.20 (m, 2H), 7.29−7.32 (m, 3H), 7.39−7.51 (m, 5H), 7.59−7.67 (m, 9H), 7.72−7.81 (m, 3H), 7.88−7.98 (m, 2H), 8.10−8.11 (m, 3H), 8.18−8.20 (m, 2H), 8.81 (d, J = 4.9 Hz, 1H), 9.10 (d, J = 4.9 Hz, 1H); ^{13}C NMR ($CDCl_3$, 75 MHz, ppm): δ 114.12, 119.53, 123.20, 126.19, 127.35, 127.46, 127.51, 127.66, 127.70, 128.06, 128.20, 128.33, 128.69, 128.76, 128.89, 130.12, 130.82, 131.13, 131.89, 132.10, 132.46, 133.31, 133.52, 134.19, 135.11, 136.38, 137.89, 138.42, 138.80, 140.56, 145.14, 145.34, 146.68, 155.00, 155.03, 155.74, 157.50, 165.12, 193.00, 213.60, 216.35, 216.47; MS (MALDI, positive): m/z 770.17 ([M−3CO]$^+$); HRMS (ESI$^+$): Found: m/z 855.18174, Calcd for $C_{54}H_{32}MnN_4O_4$ (MH^+): m/z 855.18040; Anal. Calcd for **2d**·1.4CH_2Cl_2 ($C_{55.4}H_{33.8}Cl_{2.8}MnN_4O_4$): C, 68.34; H, 3.50; N, 5.75. Found: C, 68.37; H, 3.73; N, 5.76; UV−vis−NIR (CH_2Cl_2, λ_{max}/nm, (log ε)): 908 (3.09), 828 (3.15), 502 (4.47), 356 (4.35); IR (powder, cm^{-1}, CO): 1653 (CHO), 1916, 2003, 2010.

Reactions of N-Confused Tetraphenylporphyrins with Mn(CO)$_5$Br. Preparation of 2c (Typical Procedure). A solution of 21-NO$_2$-NCTPP (**3c**) (30 mg, 45 μmol, 1.0 equiv), Mn(CO)$_5$Br (12.2 mg, 45 μmol, 1.0 equiv), and K_2CO_3 (18.6 mg, 135 μmol, 3.0 equiv) in THF (10 mL) was heated at 100 °C for 5 h under argon atmosphere. After cooling, toluene was removed under reduced pressure, and the residue was purified by silica gel column chromatography (eluent: CH_2Cl_2/hexane = 2/1). The first purple violet fraction was collected and concentrated to dryness to give **2c** in 10% yield (3.9 mg, 5 μmol). The second green fraction gave recovered **3c** in 64% yield (19.3 mg, 29 μmol).

Manganese(I) 21-Methyl N-Fused Tetraphenylporphyrinato Tricarbonyl Complex (Mn^I(21-Me-NFTPp)(CO)$_3$, ***2g****).* Starting from 21-Me-NCTPP (**3g**) (31 mg, 49 μmol, 1.0 equiv), **2g** was obtained in 43% yield (13.3 mg, 21 μmol); reaction time 2 h. ^{1}H NMR ($CDCl_3$, 300 MHz, ppm): δ 2.94 (s, 3H), 7.29 (d, J = 4.5 Hz, 1H), 7.37 (d, J = 4.8 Hz, 1H), 7.47 (d, J = 4.5 Hz, 1H), 7.52−7.61 (m, 7 H), 7.68−7.73 (m, 7H), 7.82 (d, J = 4.8 Hz, 1H), 7.86−7.89 (m, 2H), 7.97−8.01 (m, 2H), 8.27−8.29 (m, 2H), 8.52 (d, J = 5.2 Hz, 1H), 8.87 (d, J = 5.2 Hz, 1H); ^{13}C NMR ($CDCl_3$, 75 MHz, ppm): δ 16.14, 112.70, 117.97, 120.05, 124.94, 125.83, 126.24, 127.43, 127.69, 127.86, 127.88, 128.14, 128.69, 129.31, 130.70, 130.77, 131.44, 132.81, 132.85, 134.40, 135.67, 136.08, 137.85, 138.64, 138.85, 143.77, 145.43, 146.56, 152.99, 153.79, 154.04, 158.61, 165.47, 214.20, 217.20, 217.35; MS (MALDI, positive): m/z 679.91([M−3CO]$^+$); HRMS (ESI$^+$): Found: m/z 765.17236, Calcd for $C_{48}H_{30}MnN_4O_3$ (MH^+): m/z 765.16984; Anal. Calcd for **2g**·0.1CH_2Cl_2 ($C_{48.1}H_{29.2}Cl_{0.2}MnN_4O_3$): C, 74.72; H, 3.81; N, 7.25. Found: C, 74.92; H, 4.03; N, 7.16; UV−vis−NIR (CH_2Cl_2, λ_{max}/nm, (log ε)): 963 (3.19), 873 (3.26), 493 (4.55), 348 (4.53); IR (powder, cm^{-1}, CO): 1900, 1916, 2004.

Manganese(I) 21-Propyl N-Fused Tetraphenylporphyrinato Tricarbonyl Complex (Mn^I(21-Pr-NFTPp)(CO)$_3$, ***2h****).* Starting from 21-Pr-NCTPP (**3 h**) (38.0 mg, 58 μmol, 1.0 equiv), **2h** was obtained in 40% yield (18.5 mg, 23 μmol); reaction time 2 h. ^{1}H NMR ($CDCl_3$, 300 MHz, ppm): δ 0.63 (t, J = 6.9 Hz, 3H), 1.52−1.60 (m, 2H), 3.18−3.39 (m, 2H), 7.31 (d, J = 4.4 Hz, 1H), 7.40 (d, J = 4.9 Hz, 1H), 7.47 (d, J = 4.4 Hz, 1H), 7.53−7.61 (m, 6H), 7.70−7.78 (m, 7H), 7.85 (d, J = 4.9 Hz, 1H), 7.88−7.91 (m, 2H), 7.98−8.02 (m, 2H), 8.22−8.25 (m, 2H), 8.30−8.32 (m, 1H), 8.55 (d, J = 5.2 Hz, 1H), 8.87 (d, J = 5.2 Hz, 1H); ^{13}C NMR ($CDCl_3$, 75 MHz, ppm): δ 14.18, 27.10, 31.58, 113.03, 118.02, 119.96, 124.88, 125.98, 127.43, 127.60. 127.72, 127.86, 128.12, 128.65, 129.17, 130.37, 130.73, 130.82, 131.26, 131.68, 132.07, 132.85, 132.90, 134.63, 135.69, 135.85, 137.88, 138.57, 138.66, 144.04, 145.52, 146.02, 153.04, 153.81, 154.27, 158.71, 165.31, 214.05, 217.10, 217.24; MS (MALDI, positive): m/z 707.92 ([M−3CO]$^+$); HRMS (ESI$^+$): Found: m/z 793.20121, Calcd for $C_{50}H_{34}MnN_4O_3$ (MH^+): m/z 793.20114; Anal. Calcd for **2h**·0.85CH_2Cl_2 ($C_{50.85}H_{34.7}Cl_{1.7}MnN_4O_3$): C, 70.61; H, 4.04; N, 6.48. Found: C, 70.65; H, 4.16; N, 6.25; UV−vis−NIR (CH_2Cl_2, λ_{max}/nm, (log ε)): 961 (3.11), 867 (3.15), 492 (4.47), 348 (4.43); IR (powder, cm^{-1}, CO): 1904, 1915, 2002.

Manganese(I) 21-Isobutyl N-Fused Tetraphenylporphyrin-Manganese Tricarbonyl Complex (Mn^I(21-^{i}Bu-NFTPp)(CO)$_3$, ***2i****).* Starting from 21-^{i}Bu-NCTPP (**3i**) (31 mg, 46 μmol, 1.0 equiv), **2i** was obtained in 40% yield (15.0 mg, 19 μmol); reaction time 2 h. ^{1}H NMR ($CDCl_3$, 300 MHz, ppm): δ 0.49 (d, J = 6.6 Hz, 3H), 0.55 (d, J = 6.6 Hz, 3H), 1.75−1.88 (m, 1H), 3.11 (dd, J = 13.9 Hz, J = 6.1 Hz, 1H), 3.42 (dd, J = 13.9 Hz, J = 7.8 Hz, 1H), 7.32 (d, J = 4.4 Hz, 1H), 7.37 (d, J = 4.4 Hz, 1H), 7.44 (d, J = 4.9 Hz, 1 H), 7.54−7.66 (m, 7H), 7.71−7.79 (m, 7H), 7.88 (d, J = 4.9 Hz, 1H), 7.89−7.91 (m, 1H), 7.96−8.08 (m, 2H), 8.21 (d, J = 7.6 Hz, 2H), 8.30−8.57 (m, 1H), 8.56 (d, J = 5.1 Hz, 1H), 8.90 (d, J = 5.1 Hz, 1H); ^{13}C NMR ($CDCl_3$, 75 MHz, ppm): δ 14.13, 22.65, 32.76, 37.60, 113.25, 118.04, 124.92, 126.10, 127.42, 127.63, 127.80,

dx.doi.org/10.1021/ic2000393 |*Inorg. Chem.* 2011, 50, 6029–6043

127.86, 128.13, 128.65, 129.09, 130.54, 130.74, 130.87, 131.54, 132.88, 132.93, 134.63, 135.85, 137.89, 138.68, 138.75, 144.17, 145.60, 146.55, 152.96, 15381, 154.35, 158.71, 165.24, 214.03, 214.69, 217.22; MS (MALDI, positive): m/z 722.03 ($[M-3CO]^+$); HRMS (ESI^+): Found: m/z 807.21951, Calcd for $C_{51}H_{36}MnN_4O_3$ (MH^+): m/z 807.21679; Anal. Calcd for **2i**·0.4CH_2Cl_2 ($C_{51.4}H_{35.8}Cl_{0.8}MnN_4O_3$): C, 73.43; H, 4.29; N, 6.66. Found: C, 73.33; H, 4.31; N, 6.73; UV−vis−NIR (CH_2Cl_2, λ_{max}/nm, (log ε)): 960 (2.99), 869(3.09), 493 (4.33), 348 (4.30); IR (powder, cm^{-1}, CO): 1904, 1920, 2006.

*Manganese(I) 21-Isopropyl N-Fused Tetraphenylporphyrinato Tricarbonyl Complex (Mn^I(21-^{i}Pr-NFTPp)(CO)$_3$, **2j**).* Starting from 21-^{i}Pr-NCTPP (**3j**) (30 mg, 46 μmol, 1.0 equiv), **2j** was obtained in 42% yield (15.1 mg, 21 μmol); reaction time 2 h. ^{1}H NMR ($CDCl_3$, 300 MHz, ppm): δ 1.22 (d, J = 6.7 Hz, 3H), 1.48 (d, J = 7.0 Hz, 3H), 3.55 (sept, J = 6.7 Hz, J = 7.0 Hz, 1H), 7.33 (d, J = 4.58 Hz, 1H), 7.40 (d, J = 4.58 Hz, 1H), 7.46 (d, J = 4.58 Hz, 1H), 7.59−7.78 (m, 13H), 7.86 (d, J = 4.58 Hz, 1H), 7.88−7.92 (m, 2H), 7.98−8.00 (m, 4H), 8.26−8.28 (m, 1H), 8.51 (d, J = 5.2 Hz, 1H), 8.61 (d, J = 5.2 Hz, 1H); ^{13}C NMR ($CDCl_3$, 75 MHz, ppm): δ 24.00, 24.55, 27.93, 112.86, 117.85, 119.84, 124.87, 126.13, 127.34, 127.42, 127.84, 128.12, 128.41, 128.61, 129.95, 130.73, 131.08, 131.34, 131.80, 132.62, 132.87, 135.86, 136.14, 138.51, 138.66, 139.22, 145.28, 145.39, 145.52, 152.88, 153.63, 154.46, 158.79, 165.30, 204.17, 208.84, 217.15; MS (MALDI, positive): m/z = 708.07 ($[M-3CO]^+$); HRMS (ESI^+): Found: m/z 793.19896, Calcd for $C_{50}H_{34}MnN_4O_3$ (MH^+): m/z 793.20114; Anal. Calcd for **2j**·0.3CH_2Cl_2 ($C_{50.3}H_{33.6}Cl_{0.6}MnN_4O_3$): C, 73.83; H, 4.14; N, 6.85. Found: C, 73.95; H, 4.30; N, 6.63; UV−vis−NIR (CH_2Cl_2, λ_{max}/nm, (log ε)): 952 (3.27), 861 (3.30), 488 (4.64), 346 (4.63); IR (powder, cm^{-1}, CO): 1908, 1926, 2010.

*Manganese(I) 21-Benzyl N-Fused Tetraphenylporphyrinato Tricarbonyl Complex (Mn^I(21-Bn-NFTPp)(CO)$_3$, **2k**).* A THF solution of 21-benzyl NCTPP (**3k**) (41.4 mg, 59 μmol, 1.0 equiv) and K_2CO_3 (24.3 mg, 177 μmol, 3.0 equiv) was refluxed for 10 min. To the resulting mixture, a THF solution of $Mn(CO)_5Br$ (16.2 mg, 59 μmol, 1.0 equiv) was added dropwise, and the reaction mixture was refluxed for 2 h. After cooling, THF was removed under reduced pressure and residue was purified by silica gel column chromatography (eluent: CH_2Cl_2/hexane = 2/1). The first violet fraction was collected and concentrated to dryness to give **2k** in 11% yield (5.4 mg, 6.0 μmol), and the second violet fraction afforded **2d** in 2% yield (1.2 mg, 1.0 μmol). The third violet fraction gave 21-benzoyl NFTPP (**1d**) in 21% yield (8.8 mg, 12 μmol), and the fourth green fraction afforded 21-benzoyl-NCTPP (**3d**) in 19% yield (8.0 mg, 11 μmol).

^{1}H NMR ($CDCl_3$, 300 MHz, ppm): δ 4.87 (d, ^2J = 17.1 Hz, 1H), 5.01 (d, ^2J = 17.1 Hz, 1H), 6.69−6.71 (m, 2H), 6.99−7.01 (m, 2H), 7.32 (d, J = 4.4 Hz, 1H), 7.33−7.34 (m, 2H), 7.41 (d, J = 4.4 Hz, 1H) 7.45 (d, J = 4.9 Hz, 1H), 7.46−7.47 (m, 2H), 7.53−7.62 (m, 7H), 7.70−7.73 (m, 3H), 7.90 (d, J = 4.9 Hz, 1H), 7.94−8.05 (m, 5H), 8.08−8.11 (m, 2H), 8.59 (d, J = 5.1 Hz, 1H), 8.89 (d, J = 5.1 Hz, 1H); ^{13}C NMR ($CDCl_3$, 75 MHz, ppm): δ 34.07, 113.16, 118.23, 120.10, 124.88, 125.44, 126.28, 126.99, 127.23, 127.44, 127.51, 127.59, 127.71, 127.74, 127.92, 128.16, 128.29, 128.32, 128.37, 129.24, 130.30, 130.65, 130.83, 131.21, 131.59, 132.97, 133.06, 134.36, 135.84, 137.03, 138.61, 138.85, 141.66, 144.24, 145.51, 146.25, 153.31, 154.01, 154.53, 158.45, 165.23, 214.03, 216.92, 217.08; MS (MALDI, positive): m/z 756.19 ($[M-3CO]^+$); HRMS (ESI^+): Found: m/z 841.19992, Calcd for $C_{54}H_{34}MnN_4O_3$ (MH^+): m/z 841.20114; Anal. Calcd for **2k**·0.2CH_2Cl_2 ($C_{54.2}H_{33.4}Cl_{0.4}MnN_4O_3$): C, 75.89; H, 3.92; N, 6.53. Found: C, 75.84; H, 3.95; N, 6.61; UV−vis−NIR (CH_2Cl_2, λ_{max}/nm, (log ε)): 953 (3.20), 858 (3.25), 493 (4.57), 348 (4.52); IR (powder, cm^{-1}, CO): 1894, 1935, 2008.

21-Benzoyl N-Fused Tetraphenylporphyrin (21-Bz-NFTPP, 1d). ^{1}H NMR ($CDCl_3$, 300 MHz, ppm): δ 7.03−7.08 (m, 2H), 7.31−7.39 (m, 5H), 7.44−7.51 (m, 3H), 7.57−7.62 (m, 2H), 7.71−7.80 (m, 9H), 8.05−8.11 (m, 5H), 8.21−8.23 (m, 3H), 8.77 (d, J = 4.9 Hz, 1H), 9.11 (d, J = 4.9 Hz, 1H); ^{13}C NMR ($CDCl_3$, 75 MHz, ppm): δ 115.98, 119.77, 120.24, 121.01, 125.87, 126.43, 126.92, 127.55, 127.78, 127.84, 128.08, 128.27, 128.64, 128.91, 129.19, 129.57, 129.89, 131.44, 131.68, 131.90, 133.04, 133.32, 134.08, 134.51, 134.85, 134.95, 137.10, 138.67, 138.94, 140.65, 140.68, 143.02, 146.14, 147.57, 149.87, 150.09, 153.50, 156.04, 195.60; MS (MALDI, positive): m/z 716.23 ($[M]^+$); HRMS (ESI^+): Found: m/z 717.26588, Calcd for $C_{51}H_{33}N_4O$ (MH^+): m/z 717.26544; Anal. Calcd for **1d**·1.35CH_2Cl_2 ($C_{52.35}H_{34.7}Cl_{2.7}N_4O$): C, 75.62; H, 4.21; N, 6.74. Found: C, 75.38; H, 4.24; N, 6.86; UV−vis−NIR (CH_2Cl_2, λ_{max}/nm, (log ε)): 911 (3.22), 831 (3.26), 645 (3.78), 545 (4.46), 504 (4.52), 360 (4.53).

Reaction of NFTPP (1a) with $Mn_2(CO)_{10}$. A solution of **1a** (20 mg, 32 μmol, 1.0 equiv) and $Mn_2(CO)_{10}$ (7.6 mg, 19 μmol, 0.6 equiv) in 1,2-dichlorobenzene (10 mL) was heated at 130 °C for 2 h. After cooling, the solvent was removed under reduced pressure, and the residue was purified by silica gel column chromatography (eluent: CH_2Cl_2/hexane = 2/1). The first reddish purple fraction was collected and concentrated to dryness to give **2a** in 56% yield (13.4 mg, 18 μmol).

Chemical Functionalization of 2a. *Preparation of **2c** (Nitration).* Sodium nitrite (200 mg) was dissolved in 20 mL of aqueous HCl solution (3.3 wt %) and the mixture was added to a CH_2Cl_2 (10 mL) solution of **2a** (20 mg, 27 μmol). The resulting suspension was vigorously stirred at room temperature for 5 min. After neutralizing with Na_2CO_3, the organic layer was separated, dried over Na_2SO_4, and evaporated to dryness. The residue was purified by silica gel column chromatography (eluent: CH_2Cl_2/hexane = 2/1). The first purple violet fraction was collected and concentrated to dryness to give **2c** in 85% yield (18.2 mg, 23 μmol).

*Preparation of Manganese(I) 21-Formyl N-Fused Tetraphenylporphyrinato Tricarbonyl Complex (Mn^I(21-CHO-NFTPp)(CO)$_3$, **2e**) (Formylation).* A solution of Mn^I(NFTPp)(CO)$_3$ (**2a**) (40 mg, 53 μmol) in dichloromethane (10 mL) was added dropwise over 10 min to a solution of Vilsmeier−Haack regent prepared from DMF (1.78 mL, 25 mmol) and phosphorus oxychloride (2.28 mL, 26 mmol). The resulting mixture was stirred at ambient temperature for 1 h and the neutralized with aqueous $NaHCO_3$ solution. The organic layer was separated, washed with water, and dried over Na_2SO_4. After evaporation, the residue was purified by silica gel column chromatography with CH_2Cl_2. The first purple fraction was gave **2e** in 93% yield (38.2 mg, 49 μmol). ^{1}H NMR ($CDCl_3$, 300 MHz, ppm): δ 7.62−7.70 (m, 7H), 7.75−7.83 (m, 10H), 7.79−8.02 (m, 2H), 8.11−8.13 (m, 2H), 8.23 (d, J = 4.8 Hz, 1H), 8.26−8.28 (m, 2H), 8.94 (d, J = 5.1 Hz, 1H), 9.18 (d, J = 5.1 Hz, 1H), 10.14 (s, 1H); ^{13}C NMR ($CDCl_3$, 75 MHz, ppm): δ 116.74, 121.28, 122.46, 122.13, 125.25, 126.65, 127.24, 127.59, 128.20, 128.40, 128.46, 128.55, 128.98, 129.63, 130.51, 131.34, 133.28, 133.56, 133.88, 134.74, 135.17, 136.35, 136.63, 138.22, 138.71, 145.09, 147.17, 149.79, 156.10, 156.70, 156.85, 158.29, 164.22, 186.10, 213.30, 215.30, 215.58; MS (MALDI, positive): m/z 694.41 ($[M-3CO]^+$); HRMS (ESI^+): Found: m/z 779.14712, Calcd for $C_{48}H_{28}MnN_4O_4$ (MH^+): m/z 779.14910; Anal. Calcd for **2e**·0.25CH_2Cl_2 ($C_{48.25}H_{27.5}Cl_{0.5}MnN_4O_4$): C, 72.45; H, 3.47; N, 7.00. Found: C, 72.73; H, 3.52; N, 6.78; UV−vis−NIR (CH_2Cl_2, λ_{max}/nm, (log ε)): 879 (3.24), 799 (3.31), 508 (4.59), 355 (4.42); IR (powder, cm^{-1}, CO): 1640 (CHO), 1907, 1921, 2008.

*Preparation of Manganese(I) 21-Chloro N-Fused Tetraphenylporphyrinato Tricarbonyl Complex (Mn^I(21-Cl-NFTPp)(CO)$_3$, **2f**) (Chlorination).* To a CH_2Cl_2 solution of Mn^I(NFTPp)(CO)$_3$ (**2a**) (30.6 mg, 41 μmol, equiv) was added NCS (10.9 mg, 62 μmol, 1.5 equiv), and the resulting solution was stirred for 1 h. After evaporation, the residue was purified by silica gel column chromatography with CH_2Cl_2 to give **2f** in 95% yield (30.3 mg, 39 μmol). ^{1}H NMR ($CDCl_3$, 300 MHz, ppm): δ 7.38 (d, J = 4.6 Hz, 1H), 7.45 (d, J = 4.9 Hz, 1H), 7.53−7.68 (m, 2H), 7.63−7.66 (m, 6H), 7.70−7.76 (m, 8H), 7.90 (d, J = 4.9 Hz, 1H), 7.92−7.96 (m, 1H), 8.00−8.04 (m, 2H), 8.51−8.54 (m, 2H), 8.64 (d, J = 5.1 Hz, 1H), 9.02 (d, J = 5.1 Hz, 1H); ^{13}C NMR ($CDCl_3$, 75 MHz, ppm): δ: 112.16, 113.75, 118.89, 120.85, 123.85, 125.16, 127.22, 127.53, 127.99, 128.08, 128.32, 128.70, 129.27, 130.94,

Table 4. Crystal Data and Structure Analysis Results for Complexes 2a, 2h, and 2i

	2a·CH_2Cl_2	**2h**	**2i**
formula	$C_{48}H_{29}Cl_2Mn_1N_4O_3$	$C_{50}H_{33}Mn_1N_4O_3$	$C_{51}H_{35}Mn_1N_4O_3$
cryst syst	monoclinic	triclinic	triclinic
space group	$P2_1/n$ (No. 14)	$P1$	$P1$
R	0.0582	0.0874	0.0505
wR2 (all data)	0.1352	0.1900	0.1320
GOF	0.934	0.867	0.932
a (Å)	15.007(2)	10.516(2)	11.079(9)
b (Å)	12.5455(19)	12.572(3)	12.993(11)
c (Å)	21.150(3)	16.811(4)	16.504(14)
α (deg)	90	73.230(4)	67.149(17)
β (deg)	102.227(4)	78.966(4)	78.73(2)
γ (deg)	90	86.013(4)	87.872(18)
V (Å^3)	3891.6(10)	2088.5(8)	2145(3)
Z	4	2	2
T (K)	243	223	223
cryst size (mm^3)	0.2 × 0.11 × 0.02	0.22 × 0.10 × 0.08	0.40 × 0.11 × 0.10
D_{calcd} (g cm^{-3})	1.426	1.261	1.249
$2\theta_{min}$, $2\theta_{max}$(deg)	3.0, 50.2	2.58, 52.0	2.74, 52.0
no. of rflns measd (unique)	6915	8134	8402
no. of rflns measd ($I > 2\sigma(I)$)	4626	3481	5624
no. of params	523	525	564
Δ (e Å^{-3})	0.653, −0.374	0.776, −0.428	0.433, −0.267

131.21, 131.88, 132.91, 133.40, 133.54, 136.08, 136.38, 138.29, 138.87, 141.72, 143.49, 145.13, 154.36, 154.50, 154.57, 157.35, 165.84, 213.99, 216.70, 216.91; MS (MALDI, positive): m/z 700.14 ($[M-3CO]^+$), 665.16 ($[M-3CO-Cl]^+$); HRMS (ESI^+): Found: m/z 784.10991, Calcd for $C_{47}H_{26}MnClN_4O_3$ (M^+): m/z 784.10739. Anal. Calcd for **2f** ($C_{47}H_{26}ClMnN_4O_3$): C, 71.90; H, 3.34; N, 7.14. Found: C, 72.13; H, 3.37; N, 7.23; UV−vis−NIR (CH_2Cl_2, λ_{max}/nm, (log ε)): 959 (3.07), 872 (3.13), 497 (4.46), 353 (4.40); IR (powder, cm^{-1}, CO): 1909, 1919, 2010.

Demetalation Reaction of 2a. A solution of **2a** (30 mg, 39 μmol, 1.0 equiv) and $Me_3NO·2H_2O$ (38.4 mg, 350 μmol, 9.0 equiv) in toluene (5 mL) was refluxed for 30 min. After cooling, toluene was removed under reduced pressure, and the residue was purified by silica gel column chromatography (eluent: CH_2Cl_2/MeOH = 98/2). The first reddish fraction was collected and concentrated to dryness to afford **1a** in 85% yield (20.3 mg, 33 μmol).

Preparation of 21-Methyl N-Fused Tetraphenylporphyrin (21-Me-NFTPP, 1g) (Dematalation of 2g). A solution of Mn^I(21-Me-NFTPp)$(CO)_3$ (**2g**) (11.2 mg, 14 μmol, 1.0 equiv) and $Me_3NO·2H_2O$ (13.8 mg, 126 μmol, 9.0 equiv) in toluene (5 mL) was refluxed for 30 min. After cooling, toluene was removed under reduced pressure, and the residue was purified by silica gel column chromatography (eluent: CH_2Cl_2/MeOH = 97/3). The first reddish fraction was collected and concentrated to dryness to afford **1g** in 68% yield (6.2 mg, 10 μmol). ^{1}H NMR ($CDCl_3$, 300 MHz, ppm): δ 2.98 (s, 3H), 7.42 (d, J = 4.6 Hz, 1H), 7.51−7.56 (m, 1H), 7.64−7.69 (m, 7H), 7.72−7.76 (m, 6H), 7.75 (d, J = 4.3 Hz, 1H), 7.85 (d, J = 4.3 Hz, 1H), 7.91 (d, J = 4.6 Hz, 1H), 7.93−7.95 (m, 2H), 7.99−8.02 (m, 4H), 8.33−8.36 (m, 2H), 8.43 (d, J = 5.2 Hz, 1H), 8.81 (d, J = 5.2 Hz, 1H); ^{13}C NMR ($CDCl_3$, 75 MHz, ppm): δ 15.76, 114.62, 118.01, 119.30, 123.07, 123.71, 123.85, 127.07, 127.50, 127.54, 127.66, 127.93, 128.08, 128.73, 129.27, 129.96, 130.19, 131.44, 132.25, 132.95, 133.03, 133.91, 133.98, 134.96, 136.62, 138.19, 139.13, 141.06, 141.52, 146.31, 149.72, 151.20; MS (MALDI, positive): m/z 626.16 ($[M]^+$); HRMS (ESI^+): Found: m/z 627.25304, Calcd for $C_{45}H_{31}N_4(MH^+)$: m/z 627.25487; Anal. Calcd for **1g**·0.7CH_2Cl_2 ($C_{45.7}H_{31.4}Cl_{1.4}N_4$): C, 79.99; H, 4.61; N, 8.16. Found: C, 80.10; H, 4.63; N, 7.86; UV−vis−NIR (CH_2Cl_2, λ_{max}/nm, (log ε)): 970 (3.11), 879 (3.16), 697 (3.38), 642 (3.53), 538 (4.29), 494 (4.38), 362 (4.36).

X-ray Diffraction Study. Single crystal X-ray structural analysis was performed on a SMART APEX equipped with CCD detector (Bruker) using MoKα (graphite monochromated, λ = 0.71069 Å) radiation. Crystal data and crystal statistics for **2a**, **2h**, and **2i** are summarized in Table 4. The data were corrected for Lorentz, polarization, and absorption effects. The empirical absorption correction (SADABAS) was applied. The structures of **2a**, **2h**, and **2i** were solved by the direct method and refined using the SHELXL-97 program.[39] The non-hydrogen atoms were refined anisotropically by the full-matrix least-squares method. The hydrogen atoms were placed at the calculated positions.

Calculation Details. All density functional theory[30] calculations were achieved with a Gaussian03 program package.[40] The basis sets implemented in the program were used. The B3LYP density functional method[41] was used with a 631T basis set for structural optimizations and frequency calculation, and with a 6311T basis set for single-point energy calculations. The 631T bases set is composed of 6-31G** for carbon, hydrogen, nitrogen, and oxygen and TZV for manganese. The 6311T bases set is composed of 6-311++G** for carbon, hydrogen, nitrogen, and oxygen and TZV for manganese. Initial structures were based on the X-ray structures or arbitrarily constructed, and equilibrium geometries were fully optimized and verified by the frequency calculations, where no imaginary frequency was found.

■ ASSOCIATED CONTENT

Supporting Information. ^{1}H and ^{13}C NMR spectra of all new compounds and Cartesian coordinates for the optimized structures. This material is available free of charge via the Internet at http://pubs.acs.org. Crystallographic data for the structures reported in this article have been deposited with the Cambridge

Crystallographic Data Centre as supplementary publication numbers CCDC 804922 (**2a**), 804923 (**2h**), and 804924 (**2i**).

AUTHOR INFORMATION

Corresponding Author
*E-mail: hfuruta@cstf.kyushu-u.ac.jp.

ACKNOWLEDGMENT

The present work was supported by the Grant-in-Aid for Scientific Research (21750047 and 21108518) and the Global COE Program "Science for Future Molecular Systems" from the Ministry of Education, Culture, Sports, Science and Technology of Japan.

REFERENCES

(1) (a) Sessler, J. L.; Weghorn, S. J. *Expanded, Contracted, and Isomeric Porphyrins*; Elsevier: Oxford, 1997. (b) *The Porphyrin Handbook*; Kadish, K. M., Smith, K. M., Guilard, R., Eds.; Academic Press: San Diego, CA, 2000; Vol. 3. (c) *Handbook of Porphyrin Science: With Applications to Chemistry, Physics, Materials Science, Engineering, Biology and Medicine*; Kadish, K. M., Smith, K. M., Guilard, R., Eds.; World Scientific: Hackensack, NJ, 2010; Vol. 10.

(2) (a) Jasat, A.; Dolphin, D. *Chem. Rev.* **1997**, *97*, 2267–2234. (b) Sessler, J. L.; Seidel, D. *Angew. Chem., Int. Ed.* **2003**, *42*, 5134–5175. (c) Chandrashekar, T. K.; Venkatraman, S. *Acc. Chem. Res.* **2003**, *36*, 676–691. (d) Gupta, I.; Ravikanth, M. *Coord. Chem. Rev.* **2006**, *250*, 468–518. (e) Misra, R.; Chandrashekar, T. K. *Acc. Chem. Res.* **2008**, *41*, 265–279. (f) Shinokubo, H.; Osuka, A. *Chem. Commun.* **2009**, 1011–1021. (g) Shin, J.-Y.; Kim, K. S.; Yoon, M.-C.; Lim, J. M.; Yoon, Z. S.; Osuka, A.; Kim, D. *Chem. Soc. Rev.* **2010**, *39*, 2751–2767.

(3) (a) Furuta, H.; Ishizuka, T.; Osuka, A.; Ogawa, T. *J. Am. Chem. Soc.* **1999**, *121*, 2945–2946. (b) Furuta, H.; Ishizuka, T.; Osuka, A.; Ogawa, T. *J. Am. Chem. Soc.* **2000**, *122*, 5748–5757.

(4) (a) Furuta, H.; Asano, T.; Ogawa, T. *J. Am. Chem. Soc.* **1994**, *116*, 767–768. (b) Chmielewski, P. J.; Latos-Grażyński, L.; Rachlewicz, K.; Głowiak, T. *Angew. Chem., Int. Ed. Engl.* **1994**, *33*, 779–781. (c) Furuta, H.; Maeda, H.; Osuka, A. *Chem. Commun.* **2002**, 1795–1804. (d) Chmielewski, P. J.; Latos-Grażyński, L. *Coord. Chem. Rev.* **2005**, *249*, 2510–2533. (e) Morimoto, T.; Taniguchi, S.; Osuka, A.; Furuta, H. *Eur. J. Org. Chem.* **2005**, 3887–3890. (f) Srinivasan, A.; Furuta, H. *Acc. Chem. Res.* **2005**, *38*, 10–20. (g) Harvey, J. D.; Ziegler, C. *J. Inorg. Biochem.* **2006**, *100*, 869–880.(h) Toganoh, M.; Furuta, H. *Handbook of Porphyrin Science: With Applications to Chemistry, Physics, Materials Science, Engineering, Biology and Medicine*; Kadish, K. M., Smith, K. M., Guilard, R., Eds.; World Scientific: Hackensack, NJ, 2010; Vol. 2, Chapter 10.

(5) Maeda, H.; Osuka, A.; Furuta, H. *J. Am. Chem. Soc.* **2003**, *125*, 15690–15691.

(6) Toganoh, M.; Kimura, T.; Uno, H.; Furuta, H. *Angew. Chem., Int. Ed.* **2008**, *47*, 8913–8916.

(7) Gupta, I.; Srinivasan, A.; Morimoto, T.; Toganoh, M.; Furuta, H. *Angew. Chem., Int. Ed.* **2008**, *47*, 4563–4567.

(8) Shin, J.-Y.; Furuta, H.; Osuka, A. *Angew. Chem., Int. Ed.* **2001**, *40*, 619–621.

(9) Srinivasan, A.; Ishizuka, T.; Furuta, H. *Angew. Chem., Int. Ed.* **2004**, *43*, 876–879.

(10) Toganoh, M.; Furuta, H. *J. Phys. Chem. A* **2009**, *113*, 13953–13963.

(11) Ishizuka, T.; Osuka, A.; Furuta, H. *Angew. Chem., Int. Ed.* **2004**, *43*, 5077–5081.

(12) Toganoh, M.; Konagawa, J.; Furuta, H. *Inorg. Chem.* **2006**, *45*, 3852–3854.

(13) (a) Ishizuka, T.; Ikeda, S.; Toganoh, M.; Yoshida, I.; Ishikawa, Y.; Osuka, A.; Furuta, H. *Tetrahedron* **2008**, *64*, 4037−4050. (b) Toganoh, M.; Kimura, T.; Furuta, H. *Chem. Eur. J.* **2008**, *14*, 10585−10594.

(14) (a) Lee, J. S.; Lim, J. M.; Toganoh, M.; Furuta, H.; Kim, D. *Chem. Commun.* **2010**, *46*, 285–287. (b) Ikeda, S.; Toganoh, M.; Easwaramoorthi, S.; Lim, J. M.; Kim, D.; Furuta, H. *J. Org. Chem.* **2010**, *75*, 8637–8649.

(15) (a) Trofimenko, S. *J. Am. Chem. Soc.* **1966**, *88*, 1842–1844. (b) Trofimenko, S. *Chem. Rev.* **1993**, *93*, 943–980. (c) Marques, N.; Sella, A.; Takats, J. *Chem. Rev.* **2002**, *102*, 2137–2160.

(16) (a) Toganoh, M.; Ishizuka, T.; Furuta, H. *Chem. Commun.* **2004**, 2464–2465. (b) Toganoh, M.; Ikeda, S.; Furuta, H. *Inorg. Chem.* **2007**, *46*, 10003–10015.

(17) Toganoh, M.; Ikeda, S.; Furuta, H. *Chem. Commun.* **2005**, 4589–4591.

(18) (a) Toganoh, M.; Fujino, K.; Ikeda, S.; Furuta, H. *Tetrahedron Lett.* **2008**, *49*, 1488–1491. (b) Toganoh, M.; Hihara, T.; Yonekura, K.; Ishikawa, Y.; Furuta, H. *J. Porphyrins Phthalocyaninnes* **2009**, *13*, 215–222.

(19) Młodzianowska, A.; Latos-Grażyński, L.; Szterenberg, L.; Stepień, M. *Inorg. Chem.* **2007**, *46*, 6950–6957.

(20) Młodzianowska, A.; Latos-Grażyński, L.; Szterenberg, L. *Inorg. Chem.* **2008**, *47*, 6364–6374.

(21) Skonieczny, J.; Latos-Grażyński, L.; Szterenberg, L. *Inorg. Chem.* **2009**, *48*, 7394–7407.

(22) (a) Harvey, J. D.; Ziegler, C. J. *Chem. Commun.* **2002**, 1942–1943. (b) Bohle, D. S.; Chen, W.-C.; Hung, C.-H. *Inorg. Chem.* **2002**, *41*, 3334–3336. (c) Harvey, J. D.; Ziegler, C. J. *Chem. Commun.* **2003**, 2890–2891. (d) Harvey, J. D.; Ziegler, C. J.; Telser, J.; Ozarowski, A.; Krzystek, J. *Inorg. Chem.* **2005**, *44*, 4451–4453.

(23) (a) Yang, J.; N'Guessan, B. R.; Dedieu, A.; Grills, D. C.; Sun, X.-Z.; George, M. W. *Organometallics* **2009**, *28*, 3113–3122. (b) Kückmann, T. I.; Schödel, F.; Sänger, I.; Bolte, M.; Wagner, M.; Lerner, H.-W. *Organometallics* **2008**, *27*, 3272–3278.

(24) (a) Joachim, J. E.; Apostolidis, C.; Kanellakopulos, B.; Maier, R.; Marques, N.; Meyer, D.; Müller, J.; Pires de Matos, A.; Nuber, B.; Rebizant, J.; Ziegler, M. L. *J. Organomet. Chem.* **1993**, *448*, 119–129. (b) MacNeil, J. H.; Roszak, A. W.; Baird, M. C.; Preston, K. F.; Rheingold, A. L. *Organometallics* **1993**, *12*, 4402–4412.

(25) (a) Chmielewski, P. J.; Latos-Grażyński, L.; Głowiak, T. *J. Am. Chem. Soc.* **1996**, *118*, 5690–5701. (b) Schmidt, I.; Chmielewski, P. J. *Inorg. Chem.* **2003**, *42*, 5579–5593.

(26) Heating of the THF solution of 21-benzyl NCTPP (**3k**) and K_2CO_3 gave 21-benzoyl NCTPP (**3d**).

(27) (a) Ishikawa, Y.; Yoshida, I.; Akaiwa, K.; Koguchi, E.; Sasaki, T.; Furuta, H. *Chem. Lett.* **1997**, *26*, 453–454. (b) Hung, C.-H.; Liaw, C.-C.; Chin, W.-M.; Chang, G.-F.; Chuang, C.-H. *J. Porphyrins Phthalocyanines* **2006**, *10*, 953–961.

(28) Furuta, H.; Ishizuka, T.; Osuka, A.; Dejima, A.; Nakagawa, H.; Ishikawa, Y. *J. Am. Chem. Soc.* **2001**, *123*, 6207–6208.

(29) Hung, C.-H.; Ching, W.-M.; Chang, G.-F.; Chuang, C.-H.; Chu, H.-W.; Lee, W.-Z. *J. Am. Chem. Soc.* **2009**, *131*, 7952–7953.

(30) (a) Hohenberg, P.; Kohn, W. *Phys. Rev.* **1964**, *136*, B864. (b) Kohn, W.; Sham, L. J. *Phys. Rev.* **1965**, *140*, A1133–1138.

(31) Claridge, T. D. W. *High-Resolution NMR Techniques in Organic Chemistry*, 2nd ed.; Elsevier Science: Oxford, 2008.

(32) The Re(I) complex (**4a**) afforded both **2aP-3** and **2aP-6** types with a ratio of ca. 3:1 upon addition of MSA.

(33) (a) Albers, M. O.; Coville, N. *Coord. Chem. Rev.* **1984**, *53*, 227–259. (b) Luh, T.-Y. *Coord. Chem. Rev.* **1984**, *60*, 255–276.

(34) Toganoh, M.; Hihara, T.; Furuta, H. *Inorg. Chem.* **2010**, *49*, 8182–8184.

(35) The bond dissociation energies of Re−CO and Mn−CO are reported to be 179 kJ mol^{-1} and 93 kJ mol^{-1}, respectivelySkinner, H. A.; Connor, J. A. *Pure Appl. Chem.* **1985**, *57*, 79–88.

(36) Huheey, J. E.; Keiter, E. A.; Keiter, R. L. *Inorganic Chemistry—principles of structure and reactivity*, 4th ed.; Harper Collins: New York, 1993.

(37) Recently, we have succeeded to synthesize an iron(II) NFTPP complex of a double-decker ferrocene-type. Toganoh, M.; Sato, A.; Furuta, H. *Angew. Chem., Int. Ed.* **2011**, *50*, 2752–2755.

(38) (a) Geier, G. R., III; Haynes, D. M.; Lindsey, J. S. *Org. Lett.* **1999**, *1*, 1455–1458. (b) Shaw, J. L.; Garrison, S. A.; Alemán, E. A.; Ziegler, C. J.; Modarelli, D. A. *J. Org. Chem.* **2004**, *69*, 7423–7427.

(39) Sheldrick, G. M. *SHELXL-97, Program for the Solution of Crystal Structures*; University of Göttingen: Göttingen, Germany, 1997.

(40) Frisch, M. J.; Trucks, G. W.; Schlegel, H. B.; Scuseria, G. E.; Robb, M. A.; Cheeseman, J. R.; Montgomery, J. A., Jr.; Vreven, T.; Kudin, K. N.; Burant, J. C.; Millam, J. M.; Iyengar, S. S.; Tomasi, J.; Barone, V.; Mennucci, B.; Cossi, M.; Scalmani, G.; Rega, N.; Petersson, G. A.; Nakatsuji, H.; Hada, M.; Ehara, M.; Toyota, K.; Fukuda, R.; Hasegawa, J.; Ishida, M.; Nakajima, T.; Honda, Y.; Kitao, O.; Nakai, H.; Klene, M.; Li, X.; Knox, J. E.; Hratchian, H. P.; Cross, J. B.; Adamo, C.; Jaramillo, J.; Gomperts, R.; Stratmann, R. E.; Yazyev, O.; Austin, A. J.; Cammi, R.; Pomelli, C.; Ochterski, J. W.; Ayala, P. Y.; Morokuma, K.; Voth, G. A.; Salvador, P.; Dannenberg, J. J.; Zakrzewski, V. G.; Dapprich, S.; Daniels, A. D.; Strain, M. C.; Farkas, O.; Malick, D. K.; Rabuck, A. D.; Raghavachari, K.; Foresman, J. B.; Ortiz, J. V.; Cui, Q.; Baboul, A. G.; Clifford, S.; Cioslowski, J.; Stefanov, B. B.; Liu, G.; Liashenko, A.; Piskorz, P.; Komaromi, I.; Martin, R. L.; Fox, D. J.; Keith, T.; Al-Laham, M. A.; Peng, C. Y.; Nanayakkara, A.; Challacombe, M.; Gill, P. M. W.; Johnson, B.; Chen, W.; Wong, M. W.; Gonzalez, C.; Pople, J. A. *Gaussian 03*, Revision D.01; Gaussian, Inc.: Wallingford, CT, 2004.

(41) (a) Becke, A. D. *J. Phys. Chem.* **1993**, *98*, 5648. (b) Lee, C.; Yang, W.; Parr, R. G. *Phys. Rev. B* **1988**, *37*, 785. (c) Vosko, S. H.; Wilk, L.; Nusair, M. *Can. J. Phys.* **1980**, *58*, 1200. (d) Stephens, P. J.; Devlin, F. J.; Chabalowski, C. F.; Frisch, M. J. *J. Phys. Chem.* **1994**, *98*, 11623.